Supporting Information

Identification and Environmental Implications of Photo-Transformation Products of Trenbolone Acetate Metabolites

Edward P. Kolodziej,[1]* Shen Qu,[2] Kristy Forsgren,[3] Sarah A. Long,[4] James B. Gloer,[4] Gerrad Jones,[1] Daniel Schlenk,[3] Jonas Baltrusaitis,[5,6] David M. Cwiertny[2]*

[1]Department of Civil and Environmental Engineering, University of Nevada, Reno, Mail Stop 258, Reno, NV, 89557

[2]Department of Civil and Environmental Engineering, University of Iowa, 4105 Seamans Center for the Engineering Arts and Sciences, Iowa City, IA, 52242-1527

[3]Department of Environmental Sciences, University of California, Riverside, 316 Science Laboratories I, Riverside, CA, 92521

[4]Department of Chemistry, University of Iowa, E331 Chemistry Building, Iowa City, IA, 52242-1527

[5]PhotoCatalytic Synthesis Group, MESA+ Institute for Nanotechnology, Faculty of Science and Technology, University of Twente, Meander 229, P.O. Box 217, 7500 AE Enschede, The Netherlands

[6]Department of Occupational and Environmental Health, College of Public Health, University of Iowa, Iowa City, IA, 52242-1527 USA

Environmental Science and Technology

*Corresponding authors contact information:

Kolodziej: Telephone: (775) 682-5553; fax: (775) 784-1390; email: koloj@unr.edu

Department of Civil and Environmental Engineering, MS 258, 1664. N. Virginia St, Reno, NV 89557

Cwiertny: Telephone: (319) 335-1401; fax: (319) 335-5696; email: david-cwiertny@uiowa.edu

Department of Civil and Environmental Engineering, 4105 Seamans Center, University of Iowa, Iowa City, IA 52242

Contents: 38 Pages, 26 Figures, 5 Tables

Experimental: Chemicals and HR-LC/MS/MS Studies

Materials. 17α-TBOH (17α-hydroxyestra-4,9,11-trien-3-one) was obtained through BDG Synthesis (Lower Hut, NZ). 17β-TBOH (17β-hydroxyestra-4,9,11-trien-3-one) and trendione (4,9,11-estratriene-3,17-dione) were obtained from Sigma Aldrich (St. Louis, MO) and Steraloids (Newport, RI), respectively. HPLC-grade solvents were obtained from Fisher (Pittsburg, PA). If necessary, samples were extracted on 6 mL C-18 solid phase extraction cartridges (Restek, Bellefonte, PA). Stock solutions (2-10 mg/L) for each of the steroid analytes were prepared in silanized volumetric glassware, then serially diluted to create working standards. Deionized water was obtained from a Milli-Q system (Millipore, Billerica, MA, USA).

LC-HRMS/MS Separation. Though several chromatography gradients were used for separation (*e.g.*, Figures 1, 2)[24], the following separation protocol was used for most analyses of the TBA metabolites and the comparative data presented in the results and discussion section. Separations utilized a Paradigm Multi-Dimensional Liquid Chromatography (MDLC) instrument (Michrom Bioresources) using a Genesis Lightning C-18 4-µm particle, 200Å pore size (2.1 x 100 mm) column (Grace Davison). Solvent A was 0.1% acetic acid in water and solvent B contained 0.1% acetic acid in MeCN. Eluent flow rate was 200 µL/min and the solvent gradient ranged from 25% B to 72% B over 18 min, followed by 100% B for 1 min, for a 25 minute total run time.

Experimental: Nuclear Magnetic Resonance (NMR) Studies

NMR Analysis. Sample preparation for NMR required larger solution volumes and higher initial concentrations to facilitate analysis. A Suntest solar simulator was used to irradiate in parallel several (five) 100 mL solutions of 100 µM 17β-TBOH in borosilicate glass beakers. The cumulative 17β-TBOH mass in all systems was ~14 mg. After 4 h of irradiation (sufficient for 98+% transformation of 17β-TBOH parent), the entire contents of each beaker was extracted on preconditioned C-18 SPE cartridges and subsequently eluted with 2 mL of methanol. These methanol extracts from each photoreactor were then combined into one 10 mL solution used in NMR analysis. Prior to analysis, this solution was further concentrated under N_2 to reduce the methanol volume to 200 µL, freeze-dried to evaporate residual methanol, and then redissolved in a known volume of methanol prior to sample fractionation.

The concentrated product mixture was then fractionated using a Beckman System Gold HPLC with a model 166 UV detector (detection at 254 nm). The product mixture was separated into 8 fractions, 5 timed to catch individual product peaks previously identified, and 3 "catchall" fractions to assess potential formation of other peaks during the separation. This fractionation procedure utilized a Grace Apollo 5–µm C_{18} column (10 x 250 mm) and a gradient of 25–72% MeCN–H_2O over 13 minutes, 72–100% over 2 minutes, and isocratic 100% MeCN for 5 minutes at a flow rate of 2 mL/min). Product

structures present in each fraction were then assigned independently by analysis of 1D and 2D nuclear magnetic resonance (NMR) data, including ^{1}H NMR, COSY (Correlation Spectroscopy), HSQC (*Heteronuclear Single Quantum Coherence)*, and HMBC (*Heteronuclear Multiple Bond Correlation)* experiments. Two–dimensional experiments were performed on a 600–MHz Bruker AVANCE–III equipped with a 1.7–mm triple–resonance (^{1}H, ^{13}C, ^{15}N) inverse probe. Proton NMR experiments were carried out on a Bruker AVANCE 500. The isolation process yielded 12,17-dihydroxy-estra-5(10), 9(11),dien-3-one (12-hydroxy-TBOH; 2.2 mg), 10,12,17-trihydroxy-estra-4,9(11),dien-3-one (10,12-dihydroxy-TBOH; 0.7 mg), a ring-opened 11,12-dialdehyde oxidation product (TBOH-11,12-dialdehyde; 1.0 mg) 10,12-dihydroxy-trenbolone (0.7 mg), an 11,12 dialdehyde oxidation product (1.0 mg), 12-hydroxy-trenbolone (2.2 mg), and 12-methoxy-17-dihydroxy-estra-5(10), 9(11),dien-3-one (12-methoxy-TBOH; 1.1 mg), along with 2.1 mg of unreacted 17β-TBOH.

Experimental: Computational Chemistry Calculations

All calculations were performed using Gaussian 09 version B02.[3] Proposed product structures were optimized using M06-2X[1] functional in combination with 6-31+G(d,p) basis set. Geometries were optimized without any constraints followed by the vibrational frequency analysis. The absence of negative frequencies confirmed that structures were on the potential energy surface minima. UV/vis spectra were calculated using time-dependent density functional theory (TDDFT) calculated electronic transitions obtained using a large 6-311+G(2df,2p) basis set and the same functional. Calculated excitation energy values were subjected to 20 nm Lorentzian broadening to better represent experimental data. Solvation effects were simulated using the SMD model.[2]

Experimental: Ecotoxicology Studies

Medaka and in vivo exposure. Adult female Japanese medaka (*Oryzias latipes*) > 90 days old posthatch (20.35 ± 1.09 mm, 0.107 ± 0.059 g) were used from an ongoing culture at the University of California, Riverside. Fish were held in 1 L containers with carbon filtered freshwater (25 °C) with a 16:8 hour light:dark cycle. During experimentation, water quality parameters were monitored. Medaka were fed live brine shrimp (*Artemia* spp.) nauplii *ad libitum* twice daily.

Fish were exposed to the solvent carrier methanol (0.01% v/v) and nominal concentrations of 17α-TBOH, 17β-TBOH, and TBO photoproduct mixtures (predicted 10, 100, and 1000 ng/L mixture concentrations in the tank) with n = 3 independent replicates with 10 fish per replicate for each compound. After 14 days, the fish were euthanized using buffered MS-222 (250 mg/L; Sigma-Aldrich, St. Louis, MO). Fork length (cm) and weight (g) were recorded. Fish were reared and handled under an

approved protocol that followed the policies and guidelines of the University of California, Riverside Institutional Animal Care and Use Committee.

Preparation of Photolysis Product Mixtures. Solutions of each TBA metabolite were prepared in DI water to an initial concentration typically between 4-24 mg/L. These solutions were irradiated under a 1000 W Xeon arc lamp for 4 hours, which was sufficient for more than 95% transformation of the starting material. About 50 mL of the resulting photoproduct mixture was then passed through a C18 cartridge and subsequently eluted with 5-10 mL methanol. The phototransformation product mixture in methanol was stored in an amber vial at 4°C to avoid light and biodegradation until use in the ectoxicological studies.

Histological analysis. After the exposure period, five whole fish were placed in Bouin's fixative (Ricca Chemical Company, Arlington, TX) for 48-hours and then transferred to 70% ethanol. Fish were processed via a series of graded ethanol followed by xylene and infiltrated and embedded with paraffin wax. Fish were sectioned using a manual rotary microtome to a thickness of 5 µm and stained with hematoxylin and eosin (Richard Allen Scientific, Kalamazoo, MI). The ovaries were examined using a light microscope and images were captured using a digital camera attached to the microscope. Ovarian follicles were staged based on morphological characteristics previously established for teleost fishes (Lubzens et al., 2010). The percentage of primary, secondary, and vitellogenic stage follicles was quantified as: # staged follicles / # total follicles * 100.

Sex steroid analysis. Due to the small size of medaka, an insufficient amount of blood plasma could be obtained for direct measurement of sex steroids. Therefore, whole body extractions were performed (Frisch et al., 2007). Briefly, whole fish were homogenized in a buffer (100 mM phosphate buffer, 100 mM KCl, 1 mM EDTA, pH 7.4), then diethyl ether was added to the homogenate and vortexed followed by centrifugation at 3000*g* for 5 minutes. The ether supernatant was then collected, and this step was repeated twice to insure quantitative extraction. The supernatant was dried down with nitrogen in a 37 °C water bath and reconstituted with steroid assay buffer. 17β-Estradiol (E2), testosterone (T), and 11-ketotestosterone (11-KT) were measured using commercially available EIA kits following the manufacturer's protocol (Cayman Chemical, Ann Arbor, MI).

In vitro vitellogenin assay. Given the small size of medaka liver, obtaining a sufficient number of hepatocytes for primary cell culture also was not feasible. Therefore, to determine the estrogenic effects of TBA metabolite parents (Forsgren et al. in preparation) and TBA metabolite photoproducts, rainbow

trout (*Oncorhynchus mykiss*) hepatocytes were utilized. Hepatocytes were isolated from the livers of 12 fish using the protocol of Lavado *et al*. (2009). Briefly, hepatocytes were obtained using enzymatic digestion with trypsin followed by mechanical disaggregation and centrifugation using Percoll (Amersham Biosciences, Uppsala, Sweden). Hepatocytes were seeded in a 48-well culture plate with a density of $1x10^6$ cells/well with 17β-estradiol (100 ng/L) as a positive control and each of the TBA metabolite parents and photoproducts (1000 ng/L, with 5 replicate wells/treatment) were incubated with hepatocytes for 24 hours at 18 °C. After incubation, the cells were resuspended in PBS, centrifuged at 5200*g* for 5 minutes and the pellet was washed twice with PBS. The RNA was immediately isolated from the cells using a commercially available kit (SV Total RNA Isolation System, Promega, Madison, WI) following the manufacturer protocol. Vitellogenin mRNA was quantified via qPCR using iScript One-Step RT-PCR kit with SYBR Green (Bio-Rad, Hercules, CA) using the following rainbow trout primer set: tVit-364 5'-CCCACTGCTGTCTCTGAAACAG-3' (sense primer) and tVit-565 5'-GACAGTTATTGAGATCCTTGCTCTTG-3' (antisense primer). β-actin was used as a housekeeping gene using the following primer set: 5'-GTCCTTCATGATTCTCTGCTGA-3' (sense primer) and 5'-ACTCGGGTTCATTTGCATAAACA-3' (antisense primer). A total of 250 nM of each primer (vitellogenin or β-actin) was added to the 25 mL PCR reaction vial (containing SYBR Green RT-PCR Reaction Mix, 100 ng mRNA hepatocyte sample, and iScript Reverse Transcriptase for One-Step RT-PCR). Real-time reactions were performed using an iCycler-MyIQ Single Color Real-Time PCR Detection System (Bio-Rad, Hercules, CA) with the following reaction parameters: 10 min at 50 °C, 5 min at 95 °C, 40 cycles of 10 s at 95 °C, and 30 s at 56 °C with data collected at the end of each cycle. Following the amplification reaction, a melt curve analysis was determined between 60 - 95 °C with data collection at 0.1 °C intervals. The Ct was selected within the linear phase of amplification. Data analysis was performed using IQ5 (Bio-Rad, Hercules, CA). To determine the estrogenicity of the TBA metabolites and subsequent photolysis products, the estradiol equivalency (EEQ; ng/L exposure treatment response) was determined using an E2 dose-response curve calculated at various concentrations of E2 (*e.g.*, $4x10^{-12}$ M, $4x10^{-11}$ M, $4x10^{-10}$ M, $4x10^{-9}$ M, $4x10^{-8}$ M, $4x10^{-7}$ M, $4x10^{-6}$ M, and $4x10^{-5}$ M).

Statistical analysis. Statistical analyses were performed using a two-way analysis of variation (ANOVA) and a one-way ANOVA followed by a Tukey's multiple means comparison (GraphPad Prism version 5.0a for Windows, GraphPad Software, LaJolla, CA). The level of significance was determined at $p < 0.05$ for all statistical analyses.

Additional Ecotoxicology Results

Histological analysis. For the *in vivo* medaka treatment with 17α-TBOH photoproducts at the lowest concentration (10 ng/L) for a 14 day exposure, no significant ($p > 0.05$) difference in the composition and percentage of ovarian follicles in medaka was observed (Figure 4). However, there was a significant difference ($p = 0.008$, $p = 0.0018$ respectively) in ovarian composition in medaka exposed to 100 ng/L and 1000 ng/L 17α-TBOH photoproducts for 14 days. Similarly, medaka exposed to 100 ng/L 17α-TBOH photoproducts had ovaries with significantly ($p = 0.0031$) more vitellogenic stage follicles compared to other TBA metabolite photoproduct treatments (primary stage $p = 0.3217$, secondary stage $p = 0.8411$; Figure 4B). The percentage of primary ovarian follicles also were significantly ($p = 0.038$) reduced in the ovaries of medaka exposed to 1000 ng/L 17α-TBOH photoproducts and had a significant ($p = 0.0351$) increase in vitellogenic ovarian follicles (Figure 4C).

Sex steroid levels. Medaka treated with 17α-TBOH photoproducts for 14 days had significant ($p < 0.0001$) reductions in whole body E2 levels (pg/mg; Figure 5A) at the two highest mixture doses. 17β-estradiol significantly ($p = 0.0053$) decreased in fish with increasing concentrations of 17α-TBOH photoproducts. Most interestingly, though a trend upward is observed, no difference ($p = 0.1691$) in whole body E2 levels was observed after exposure to 17β-TBOH photoproducts; while a trend upward also is observed, a significant ($p = 0.0473$) increase in E2 levels was observed after exposure to TBO photoproducts (Figure 5A). Unlike effects observed for the TBO parent, the TBO photolysis product mixtures did not significantly alter androgen levels in medaka (T: $p = 0.4920$ and 11-KT: $p = 0.1755$; Figure 5).

In vitro vitellogenin assay. An *in vitro* analysis to quantify the production of vitellogenin mRNA incubated with 1000 ng/L TBA metabolite photoproducts in rainbow trout hepatocytes was used to determine the overall E2 equivalency (ng/L) as a measure of the estrogenicity of the photoproduct mixtures. All TBA metabolite photolysis product mixtures showed some estrogenic properties (Figure S26). 17α-TBOH photolysis products exhibited the greatest relative *in vitro* estrogenic activity (4.25 ± 0.06 ng/L) followed by TBO photolysis products (3.43 ± 0.04 ng/L) and 17β-TBOH photolysis products (3.00 ± 0.01 ng/L; Figure S26).

References for Computational Chemistry

(1) Zhao, Y.; Truhlar, D. *Theoretical Chemistry Accounts* **2008**, *120*, 215.

(2) Marenich, A. V.; Cramer, C. J.; Truhlar, D. G. *The Journal of Physical Chemistry B* **2009**, *113*, 6378.

(3) Frisch, M. J.; Trucks, G. W.; Schlegel, H. B.; Scuseria, G. E.; Robb, M. A.; Cheeseman, J. R.; Scalmani, G.; Barone, V.; Mennucci, B.; Petersson, G. A.; Nakatsuji, H.; Caricato, M.; Li, X.; Hratchian, H. P.; Izmaylov, A. F.; Bloino, J.; Zheng, G.; Sonnenberg, J. L.; Hada, M.; Ehara, M.; Toyota, K.; Fukuda, R.; Hasegawa, J.; Ishida, M.; T. Nakajima, Y. H., O. Kitao, H. Nakai, T. Vreven, J. A. Montgomery, Jr., J. E. Peralta, F. Ogliaro, M. Bearpark, J. J. Heyd, E. Brothers, K. N. Kudin, V. N. Staroverov, R. Kobayashi, J. Normand, K. Raghavachari, A. Rendell, J. C. Burant, S. S. Iyengar, J. Tomasi, M. Cossi, N. Rega, J. M. Millam, M. Klene, J. E. Knox, J. B. Cross, V. Bakken, C. Adamo, J. Jaramillo, R. Gomperts, R. E. Stratmann, O. Yazyev, A. J. Austin, R. Cammi, C. Pomelli, J. W. Ochterski, R. L. Martin, K. Morokuma, V. G. Zakrzewski, G. A. Voth, P. Salvador, J. J. Dannenberg, S. Dapprich, A. D. Daniels, ; O. Farkas, J. B. F., J. V. Ortiz, J. Cioslowski, D. J. Fox. Gaussian 09, Revision B.02 Gaussian, Inc., Wallingford CT, 2009.

Table S1: Observed MS/MS fragments for 17α-TBOH, 17β-TBOH and trendione standards used for identification of photoproducts. Although high resolution FT-MS detection was used for full scan spectra, low resolution IT-MS detection was employed for all MS/MS data, reducing the mass precision observed for these fragments to unit resolution.

	17α-TBOH *m/z*	**17β-TBOH *m/z***	**Trendione *m/z***
Predicted $[M+H]^+$ Exact Mass	271.1698	271.1698	269.1541
Observed $[M+H]^+$ Mass (FT-MS)	271.1681	271.1681	269.1523
MS/MS Fragments (IT-MS)	253	253	251
	243	235	233
	225	227	225
	211	211	207
	197	197	195
	183	185	
		179	169
	159	***159***	***159***
	147	145	143
	133	***133***	***133***

Table S2: NMR Data for 17β-TBOH in deuterated methanol (CD_3OD).

Position	δ_H[a] (mult., J_{HH})	δ_C[b]	HMBC[c] (H→C#)
1	2.80 (ddt, 1.7, 7.2, 17) 2.88 (ddt, 1.7, 7.2, 17)	25.0	2, 3, 5, 9, 10
2	2.43 (t, 7.2)	37.0	1, 3, 4, 10
3		202.0	
4	5.75 (s)	123.2	2, 6, 10
5		160.1	
6	2.61 (m)	32.3	4, 5, 7, 10[e]
7	1.28 (dq, 5.7, 12) 1.93 (dq, 4, 12)	27.8	5, 6, 8, 9
8	2.47 (m)	38.9	6, 9, 10, 15
9		144.4	
10		127.8	
11	6.54 (d, 9.9)	124.2	8,[e] 9, 10, 12, 13
12	6.49 (d, 9.9)	144.2	5,[de] 9, 13, 14, 17, 18
13		46.6	
14	1.46 (m)	48.8	8, 13, 15, 16, 17, 18[e]
15	1.45 (m) 1.70 (m)	23.6	8,[e] 13, 14, 17, 18[de]
16	1.56 (m) 2.09 (m)	30.0	14, 15 13, 14, 17
17	3.81 (dd, 9.0, 8.0)	77.8	12, 13, 15,[e] 16, 18
18	0.90 (s)	13.7	12, 13, 14, 17

[a]500 MHz. [b]150 MHz. [c]600 MHz. [d]Four-bond or five-bond coupling. [e]Weak correlation.

Table S3: NMR Data for 10,12-dihydroxy-trenbolone in deuterated methanol (CD_3OD).

Position	δ_H[a] (mult., J_{HH})	δ_C[b]	HMBC[c] (H→C#)
1	2.26 (ddd, 4.0, 8.7, 14) 2.42 (ddd 4.4, 8.7, 14)	33.4	2, 3, 5, 9, 10 2, 3, 5, 10
2	2.47 (ddd, 4.4, 8.7, 13) 2.58 (ddd, 4.0, 8.7, 13)	35.2	3, 10 1, 3, 10
3		201.3	
4	5.78 (d, 1.4)	124.7	2, 6, 10
5		168.2	
6	2.31 (ddd, 3.1, 3.6, 13) 2.87 (m)	31.9	5 4, 5, 7
7 ax 7 eq	1.12 (dq, 3.9, 13) 2.11 (m)	33.4	
8	2.40 (m)	38.2	
9		146.3	
10		70.8	
11	6.02 (dd; 5.7, 2.0)	123.7	8, 10, 13
12	3.84 (d, 5.7)	69.6	9, 11, 14, 18
13		46.3	
14	1.49 (ddd, 7.3, 10, 11)	42	8, 18
15	1.40 (dq, 5.1, 12) 1.80 (m)	24.4	8, 14 14
16	1.58 (m) 2.03 (dddd, 4.0, 5.1, 9.2, 13)	30.0	 13, 17
17	4.26 (t, 9.0)	73.6	13, 18
18	0.75 (s)	10.4	12, 13, 14, 17

[a]500 MHz. [b]150 MHz. [c]600 MHz

Table S4: NMR Data for 11,12-dialdehyde-trenbolone product in deuterated methanol (CD_3OD).

Position	δ_H[a] (mult., J_{HH})	δ_C[b]	HMBC[c] (H→C#)
1	2.70 (ddd, 6.2, 13, 15) 3.61 (ddd; 3.4, 4.8, 15)	25.1	3, 5, 10
2	2.45 (dq, 0.7, 8) 2.59 (m)	37.3	1, 3, 4 10
3		200.1	
4	6.08 (br s)	130	10
5		156.1	
6	2.60 (m) 2.90 (dddd, 2.0, 5.8, 14, 20)	25.5	
7	1.44 (ddt, 4.0, 6.4, 14) 1.90 (m)	24.4	6, 14
8	3.00 (dt, 4.0, 11)	31.7	6, 9
9		144.7	
10		147.8	
11	9.99 (s)	190.8	8, 9
12	9.13 (s)	207.7	13, 18
13		60.2	
14	2.15 (m)	46.7	16
15	1.61 (m) 1.94 (m)	26.5	16 13
16	1.60 (m) 2.11 (m)	30.0	13, 17
17	4.21 (t, 8.5)	76.6	12, 16
18	1.01 (s)	6	12, 13, 14, 17

[a]500 MHz. [b]150 MHz. [c]600 MHz

Table S5: NMR Data for 12-hydroxy-trenbolone and 12-methoxy-trenbolone products in deuterated methanol (CD_3OD).

	12-hydroxy-trenbolone			**12-methoxy-TB**
Position	δ_H[a] (mult., J_{HH})	δ_C[b]	HMBC[c] (H→C#)	δ_H[a] (mult., J_{HH})
1	2.52 (m) 2.75 (m)	26.5	2, 3, 5, 10 3, 5, 10	2.53 (m) 2.77 (m)
2	2.51 (m)	39.3	1, 10	2.53 (m)
3		212.5		
4	2.91 (m)	45.3		2.91 (m)
5		133.8		
6	2.01 (m) 2.27 (m)	31.3	5, 7, 8, 10	2.03 (m) 2.27 (m)
7	1.27 (dq, 5.1, 12) 1.91 (m)	28.0	6, 8, 9, 14 5, 9	1.24 (dq, 5.3, 12) 1.90 (m)
8	1.94 (m)	39.5	9	1.95 (m)
9		140.5		
10		128.3		
11	5.77 (d, 5.3)	121.0	8, 10, 12, 13	5.88 (d, 5.4)
12	3.89 (d, 5.3)	70.3	9, 11, 13, 14, 18	3.51 (d, 5.4)
12-OMe				3.47 (s)
13		46.4		
14	1.56 (m)	41.3	8, 12, 13, 18	1.57 (m)
15	1.41 (dq, 5.2, 12) 1.79 (dddd, 4.2, 8.2, 9.6, 12)	24.2	8, 13, 14, 16	1.39 (dq, 5.3, 12) 1.79 (dddd, 4.1, 8.2, 9.6, 12)
16	1.55 (m) 2.02 (m)	29.9	13, 14, 17	1.56 (m) 2.04 (m)
17	4.30 (t, 9.0)	73.9	16	4.27 (t, 9.2)
18	0.71 (s)	10.9	12, 13, 14, 17	0.73 (s)

[a]500 MHz. [b]150 MHz. [c]600 MHz.

Figures: HPLC-DAD and LC-HRMS/MS Chromatograms, Spectra, NMR, and Ecotoxicology Data

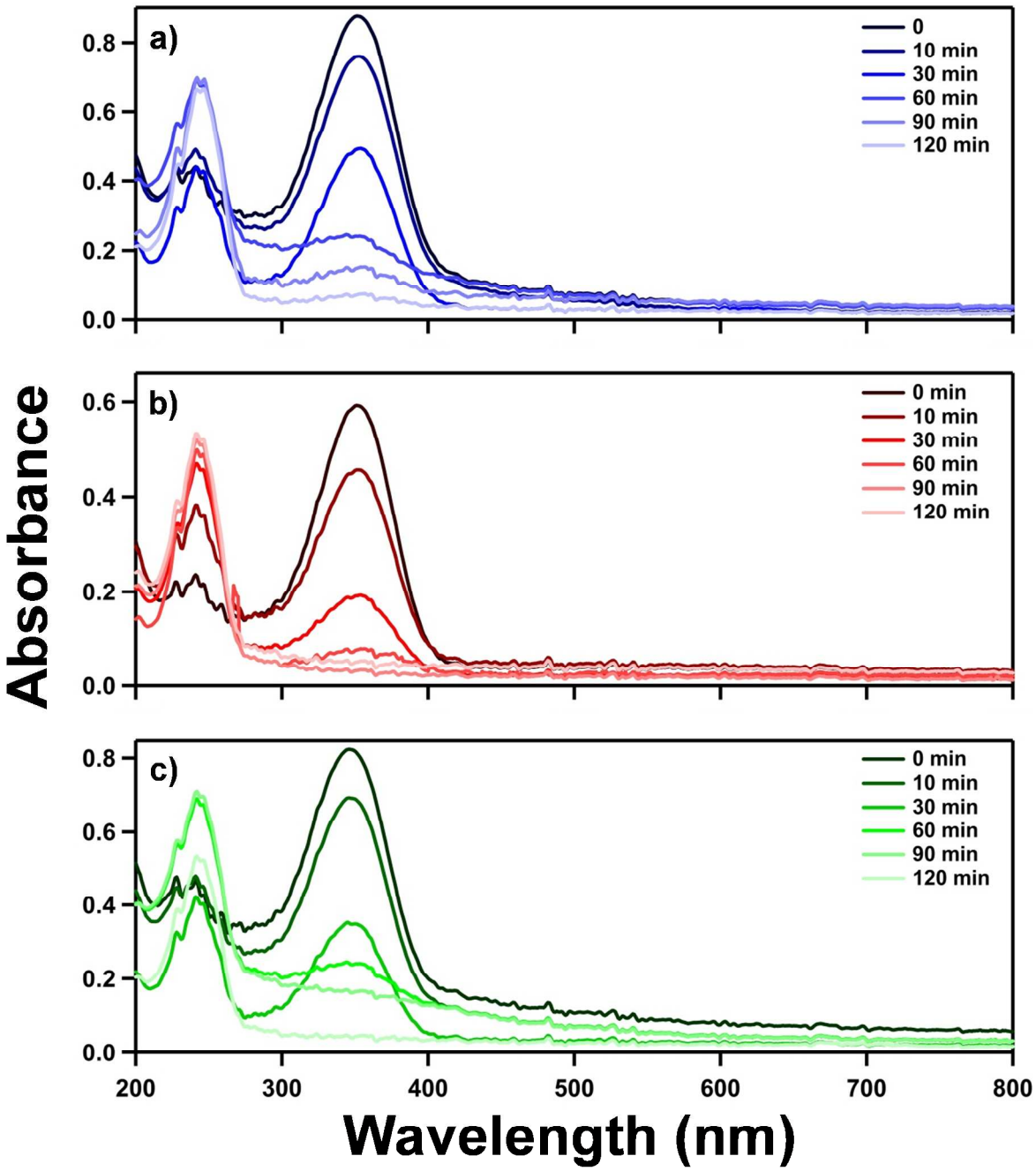

Figure S1: UV/vis absorbance scans for 10 μM solutions of (a) 17α-TBOH, (b) 17β-TBOH and (c) TBO as a function of irradiation time.

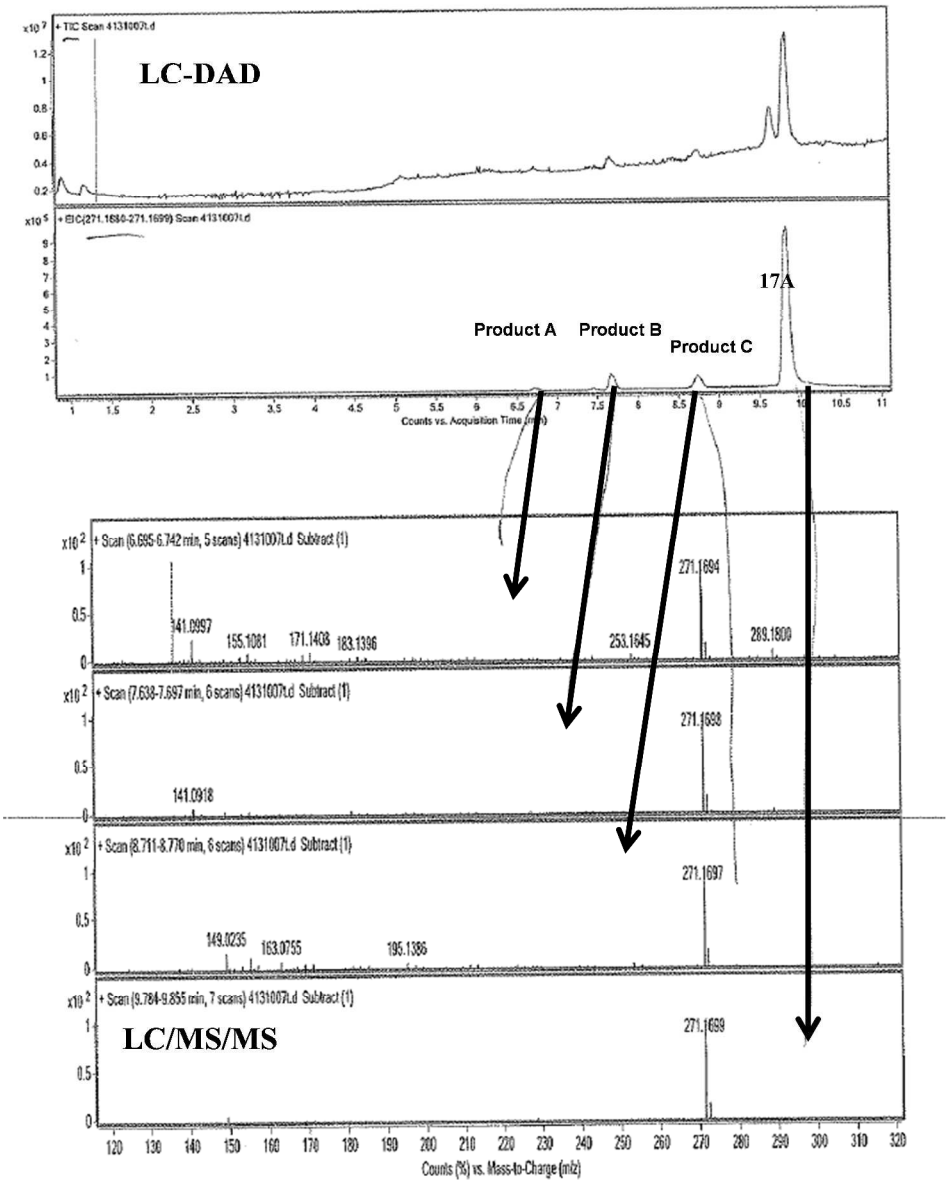

Figure S2: LC-DAD and LC/MS/MS (not the high resolution Orbitrap instrument) analysis of 17α-TBOH and photoproducts after irradiation. Note the slight m/z 289 peaks observed for the first two products. These m/z 289 peaks were not observed in the LC-HRMS/MS analysis, leading us to conclude that we observed $[M+H-H_2O]^+$ ions with the Orbitrap.

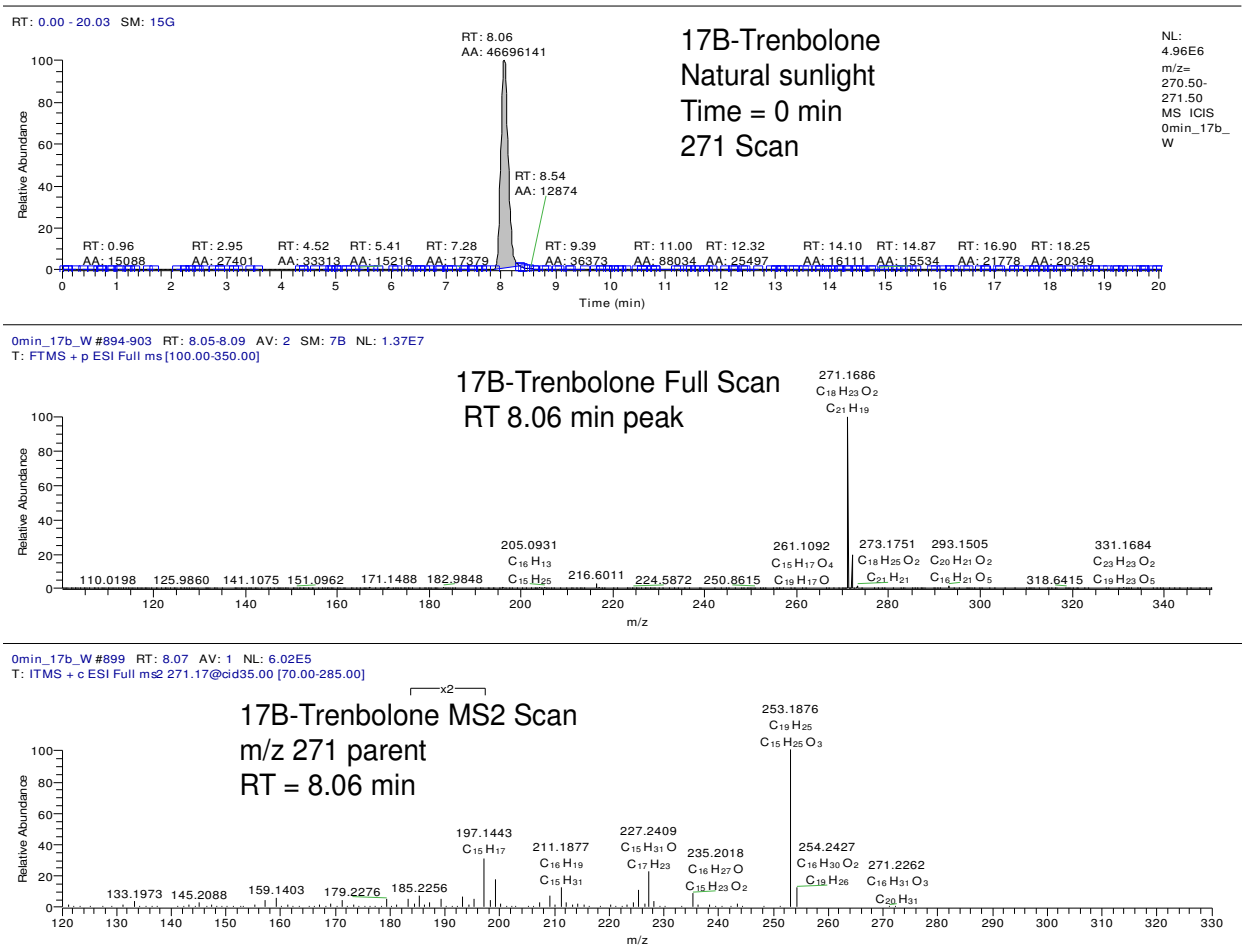

Figure S3: Initial 17β-TBOH parent chromatogram, full scan spectra, and MS/MS spectra prior to initiating the photolysis experiment. For this figure, and all other LC-HRMS/MS figures (Figures S3-S20), the high resolution MS detector (FTMS) was only used for the full scan spectra, while the lower resolution ITMS detector was used for the MS/MS data collection. Thus, the MS2 scans are lower resolution than presented, only having unit resolution for MS/MS fragments.

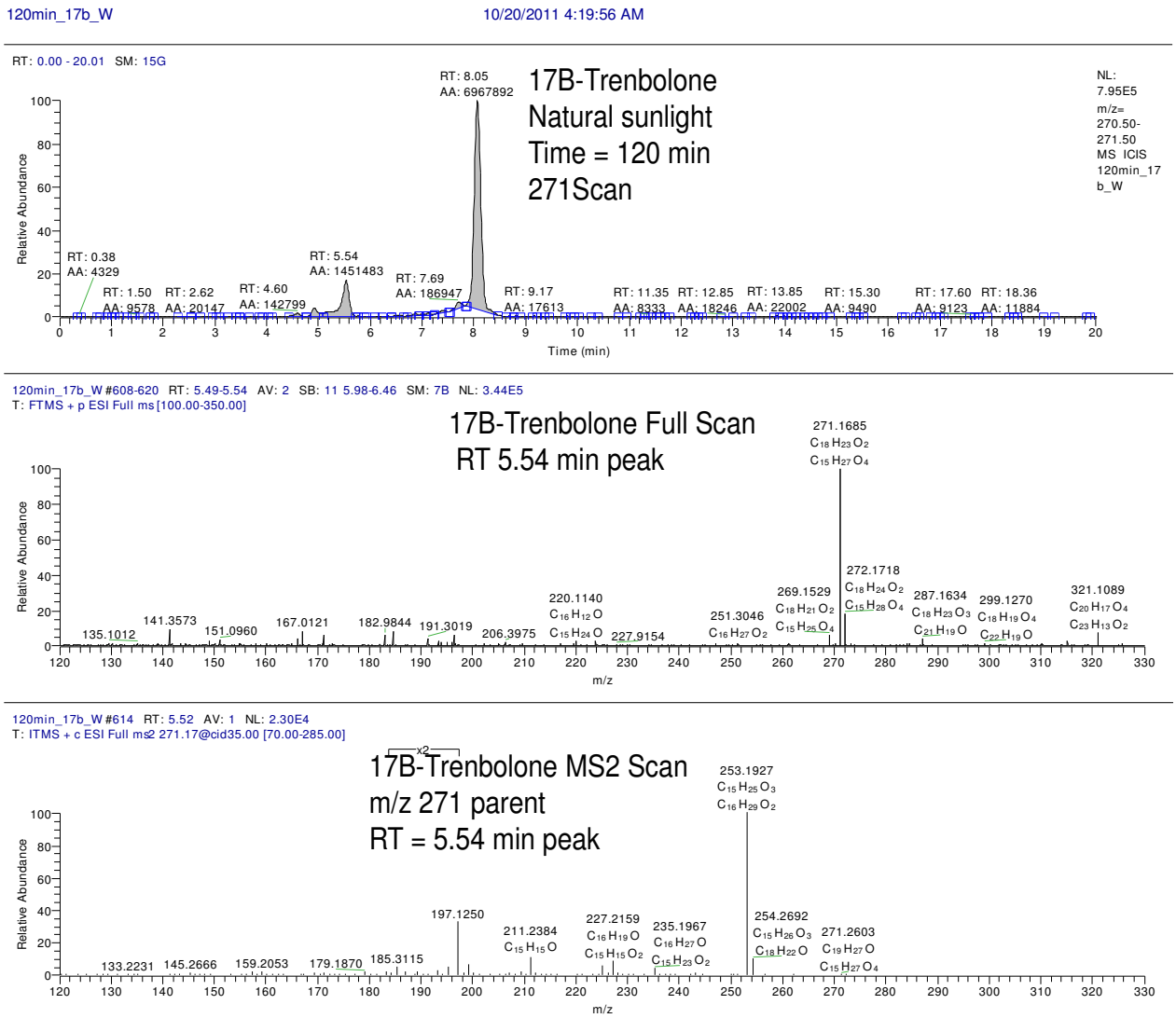

Figure S4: Observed 17β-TBOH product chromatogram, full scan spectra, and MS/MS spectra after 120 minutes of irradiation. Monohydroxy product peaks ($[M+H-H_2O]^+$ ions) are observed at 4.93, 5.54, and 7.69 minutes, with the dominant 12-hydroxy product at 5.54 minutes. Note the similar full scan and MS/MS scans observed for these products as compared to 17β-TBOH in Figure S3 and Figure 1.

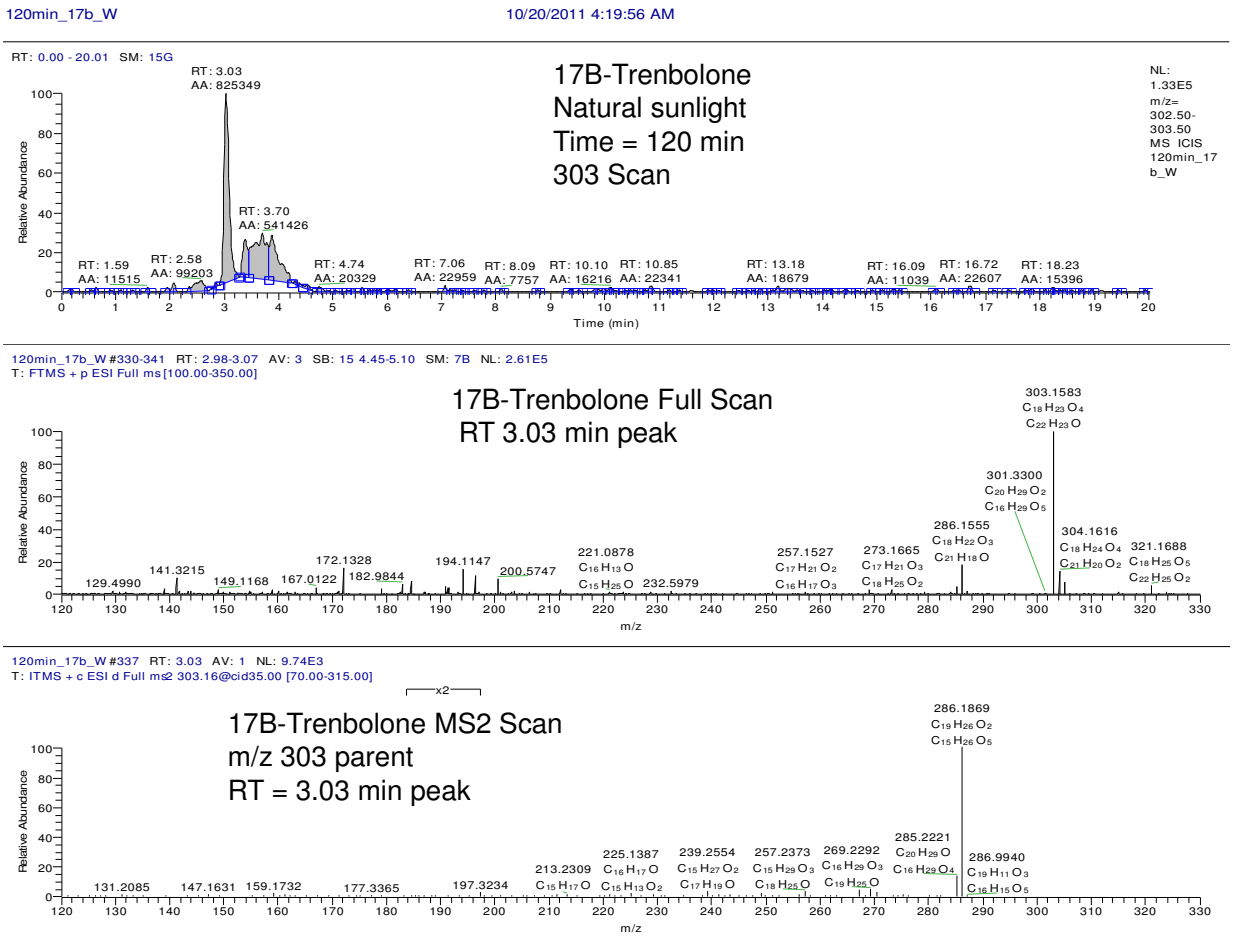

Figure S5: Observed 17β-TBOH product chromatogram, full scan spectra, and MS/MS spectra after 120 minutes of irradiation. The poorly resolved m/z 303 peaks observed at 3-4 minute retention times likely represent secondary and tertiary dialdehyde or dihydroxy products.

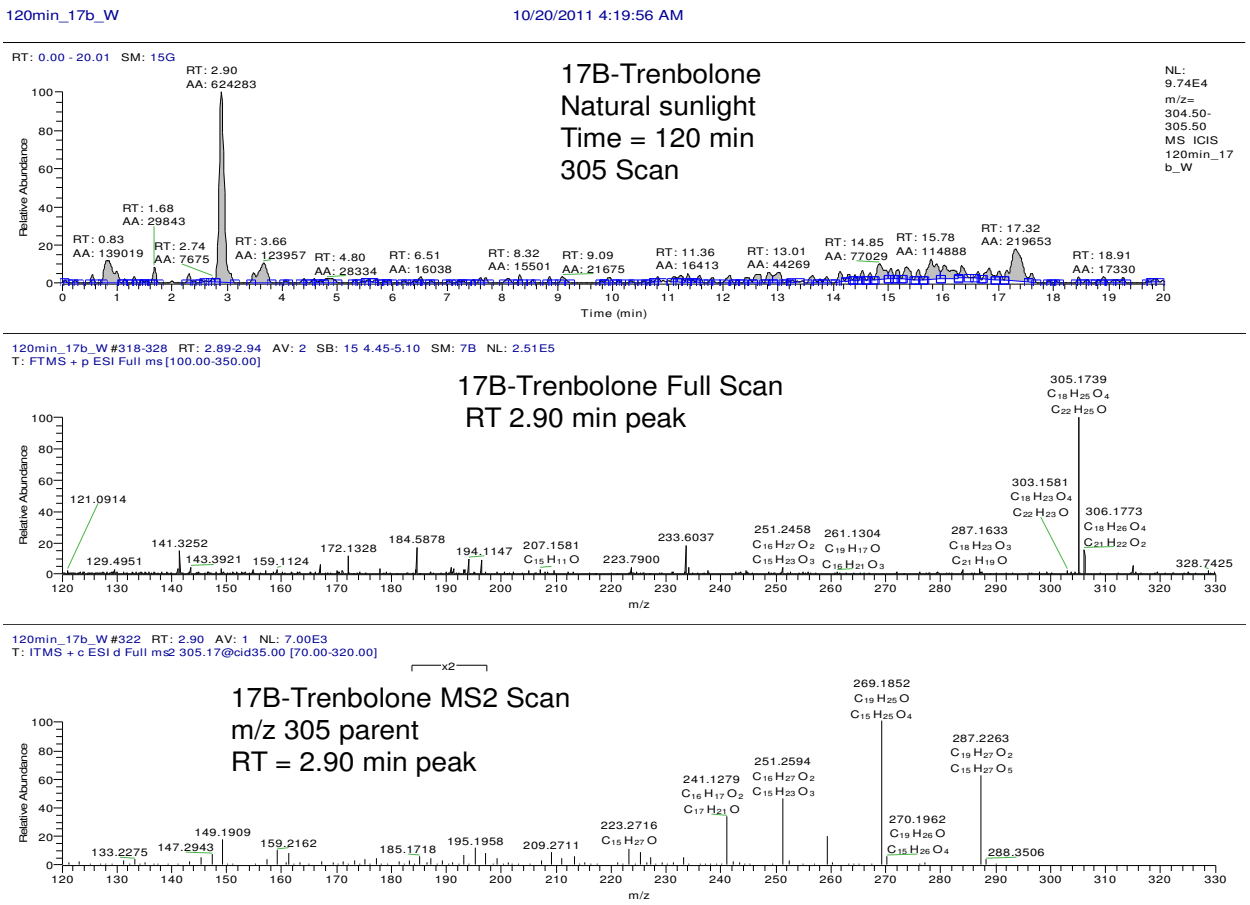

Figure S6: Observed 17β-TBOH product chromatogram, full scan spectra, and MS/MS spectra after 120 minutes of irradiation. Based on the results of the NMR analysis, we propose that the m/z 305 peak at 2.90 minutes represents 10,12-dihydroxy-trenbolone.

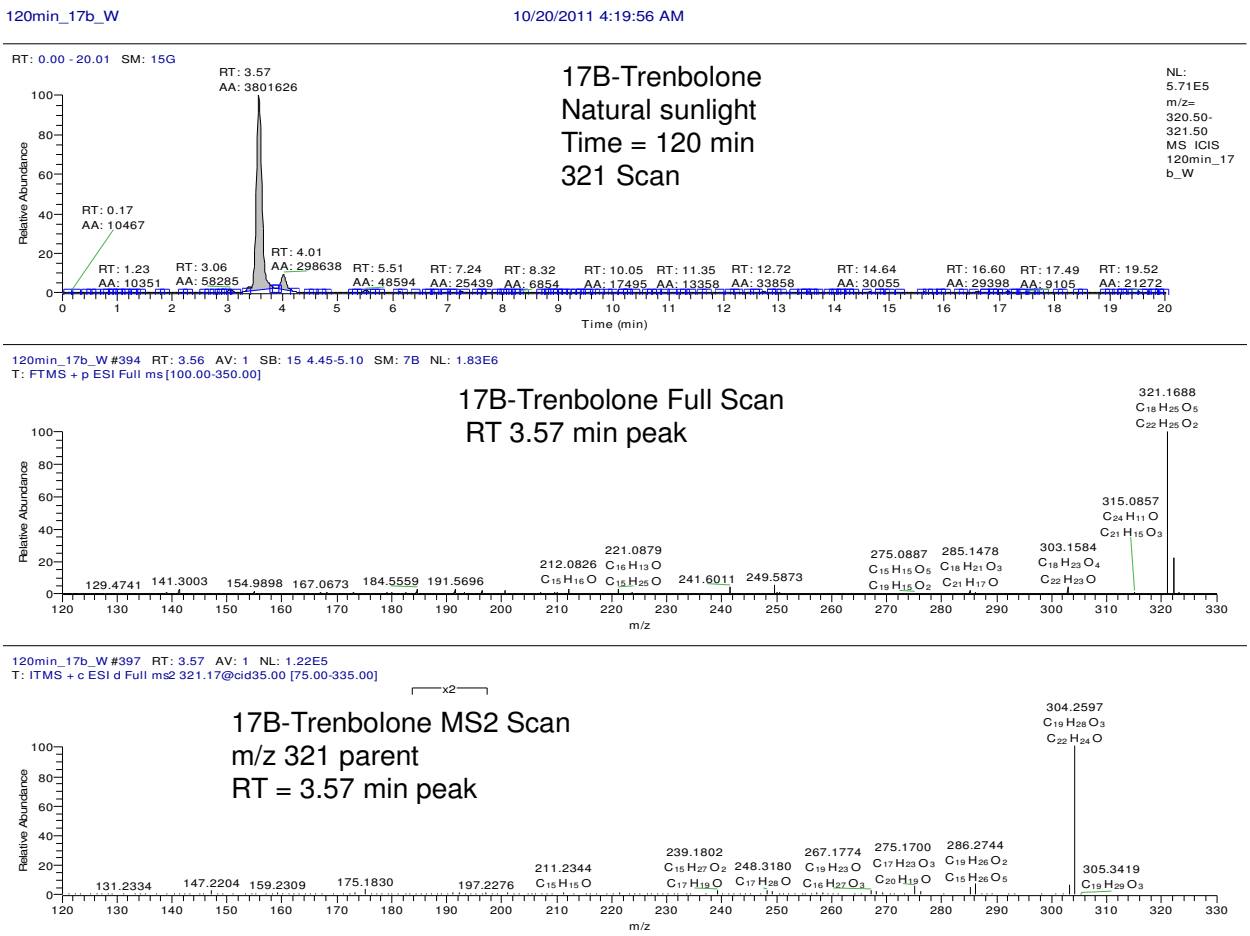

Figure S7: Observed 17β-TBOH product chromatogram, full scan spectra, and MS/MS spectra after 120 minutes of irradiation. The m/z 321 peaks at 3.57 and 4.01 minutes are presumably trihydroxy-trenbolone species.

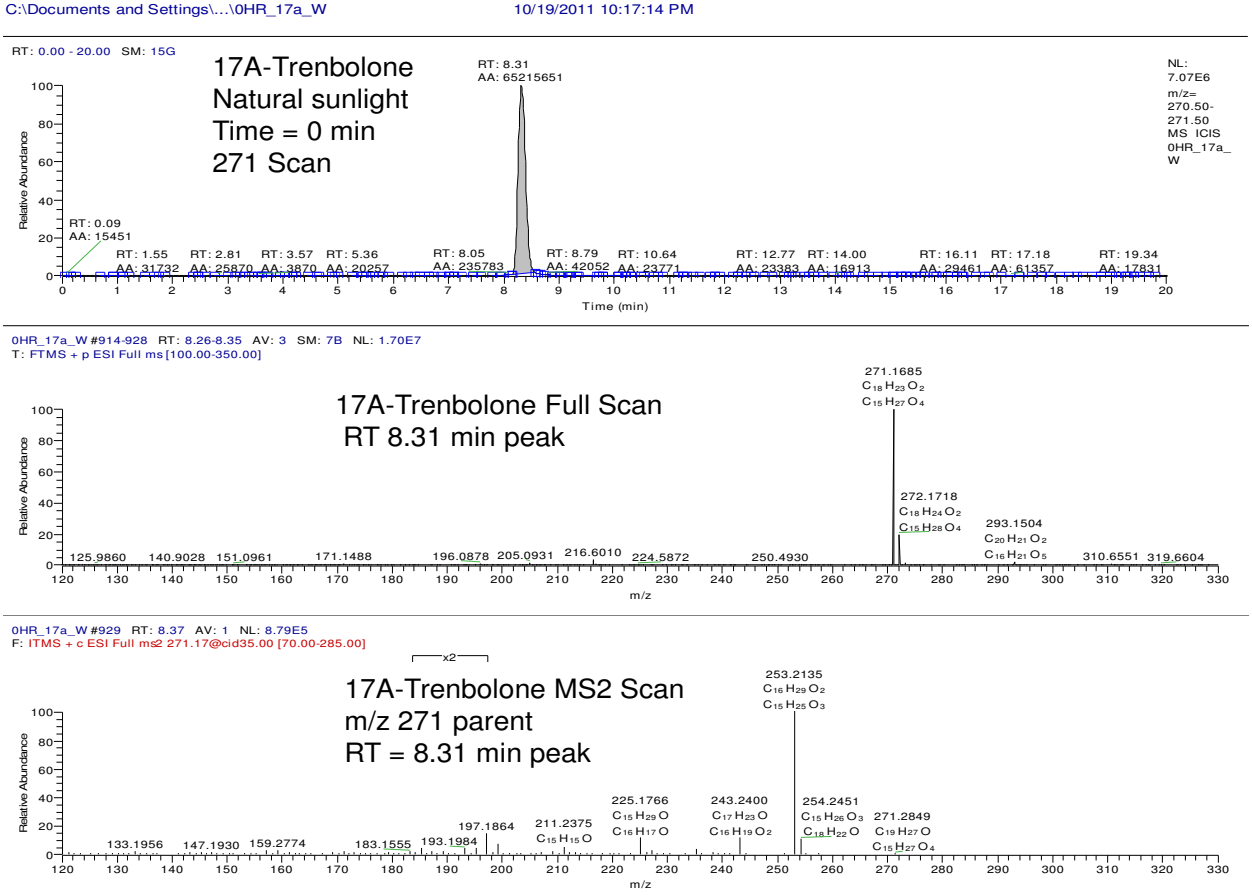

Figure S8: Initial 17α-TBOH parent chromatogram, full scan spectra, and MS/MS spectra prior to initiating the photolysis experiment.

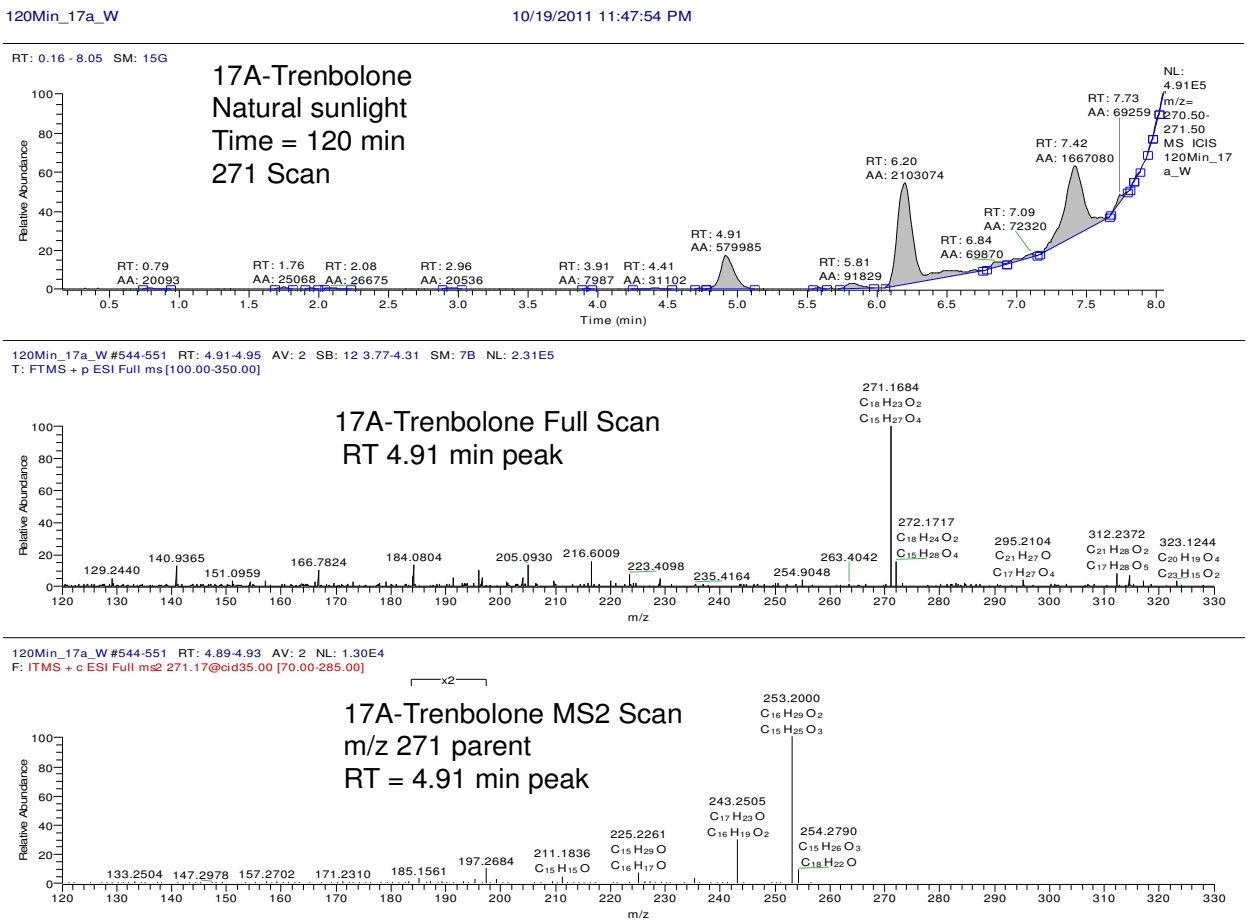

Figure S9: Observed 17α-TBOH product chromatogram, full scan spectra, and MS/MS spectra after 120 minutes of irradiation for the m/z 271 peak at 4.91 minutes. Monohydroxy product peaks ($[M+H-H_2O]^+$ ions) are observed at 4.91, 6.20, and possibly 7.42 minutes. By analogy with 17β-TBOH products, we propose that the 6.20 minute peak is the dominant 12-hydroxy product, with the 10-hydroxy product at 4.91 minutes.

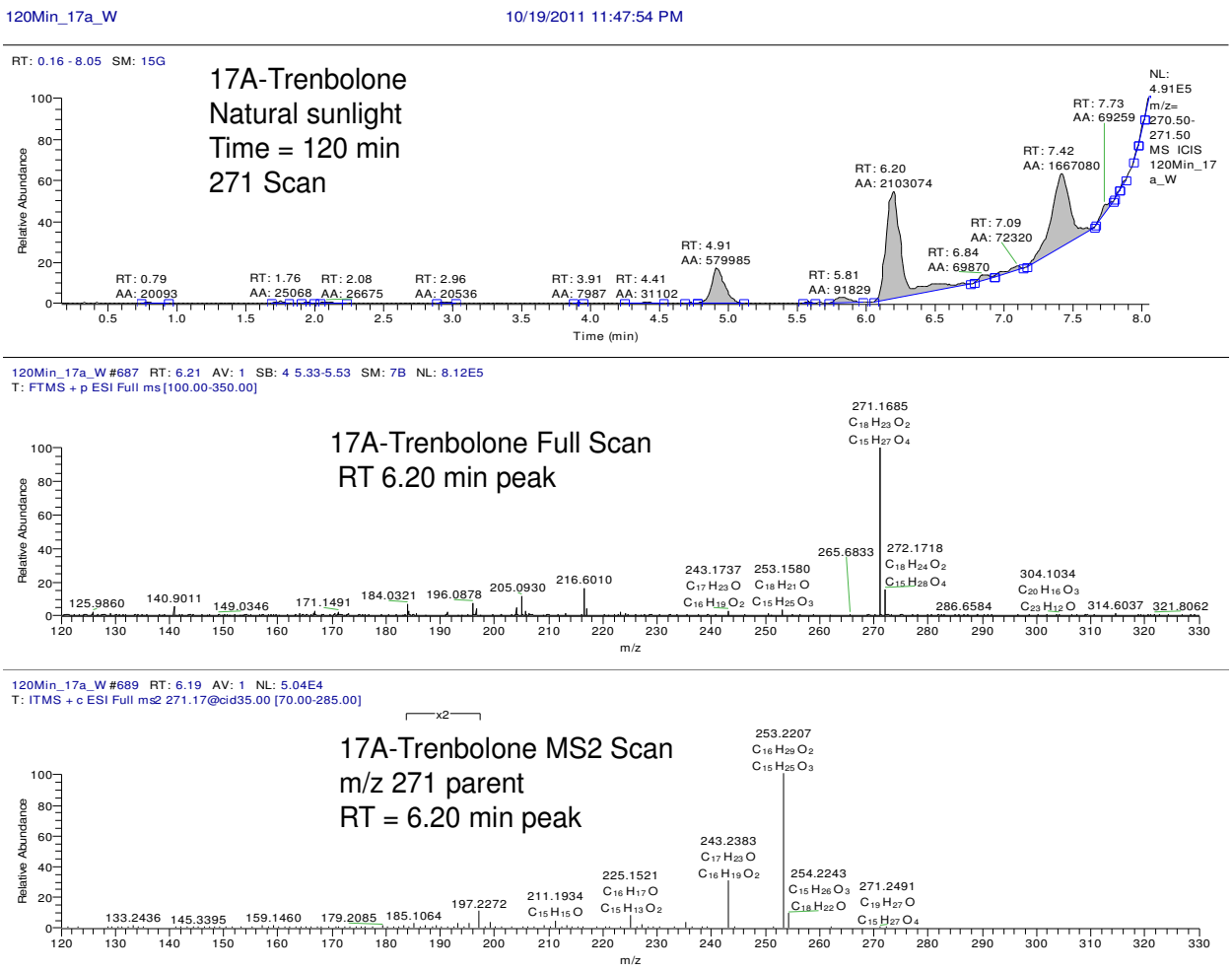

Figure S10: Observed 17α-TBOH product chromatogram, full scan spectra, and MS/MS spectra after 120 minutes of irradiation for the dominant m/z 271 peak at 6.20 minutes.

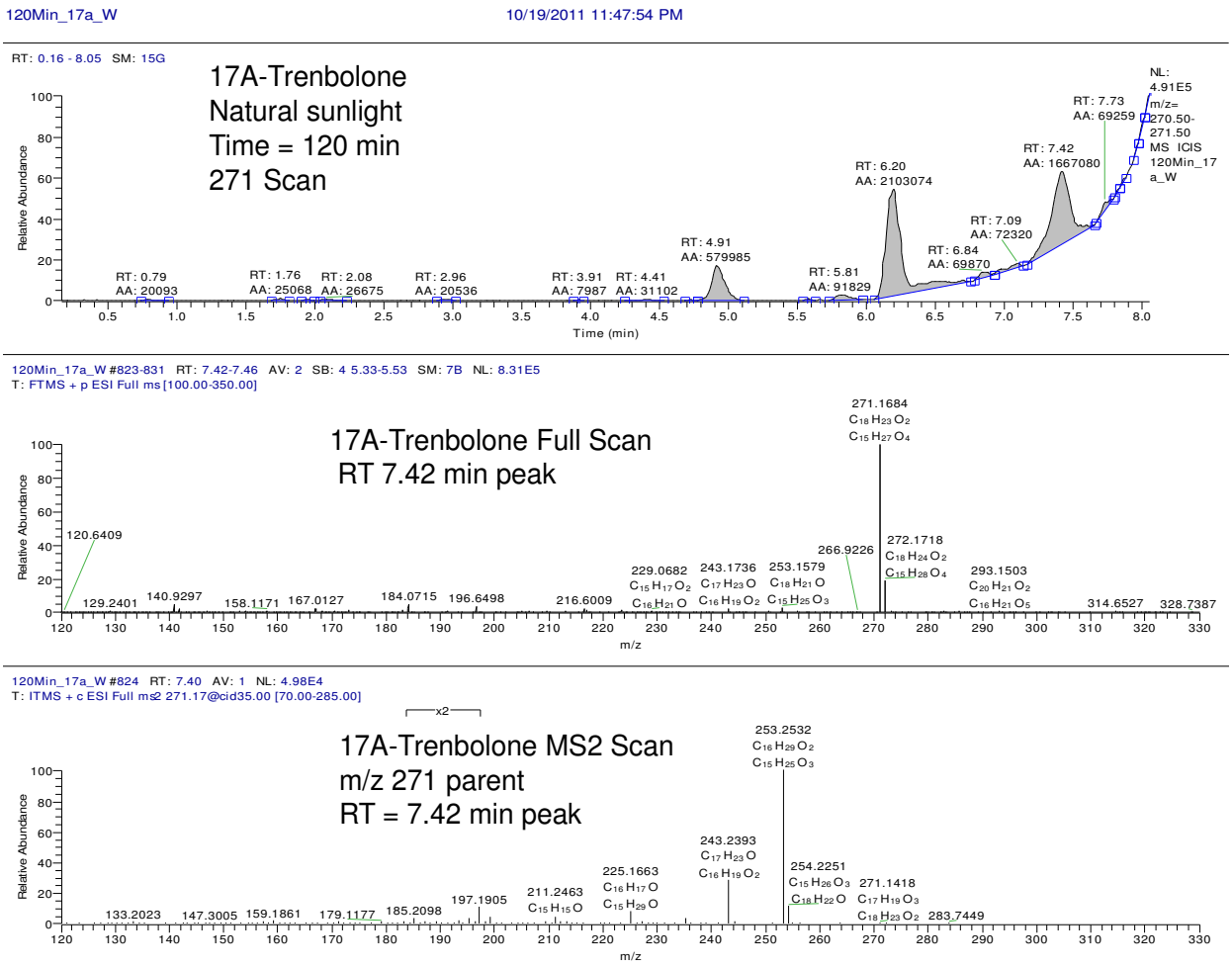

Figure S11: Observed 17α-TBOH product chromatogram, full scan spectra, and MS/MS spectra after 120 minutes of irradiation for the m/z 271 peak at 7.42 minutes. Due to its proximity to the 17α-TBOH parent at 8.31 minutes, this may represent a $[M+H]^+$ ion of a 17α-TBOH stereoisomer or structural analog, although it could also be a $[M+H-H_2O]^+$ ion of another uncharacterized hydroxy-trenbolone product.

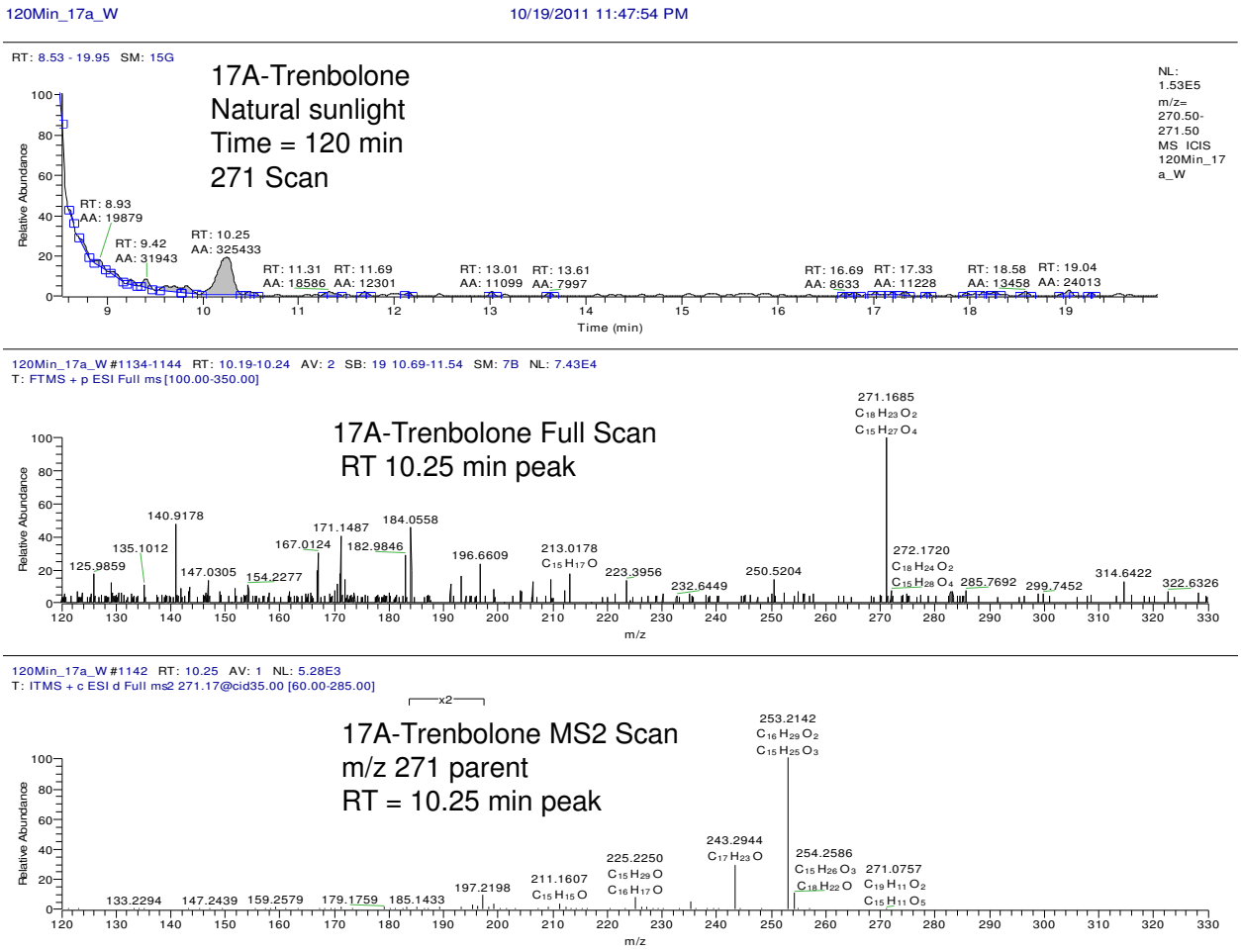

Figure S12: Observed 17α-TBOH product chromatogram, full scan spectra, and MS/MS spectra after 120 minutes of irradiation for the m/z 271 peak at 10.25 minutes. Due to its much later retention time, suggesting decreased polarity relative to the parent 17α-TBOH at 8.31 minutes retention time, we suggest that this product is likely a structural analog or stereoisomer of 17α-TBOH. However, this product has not been isolated and further characterized structurally.

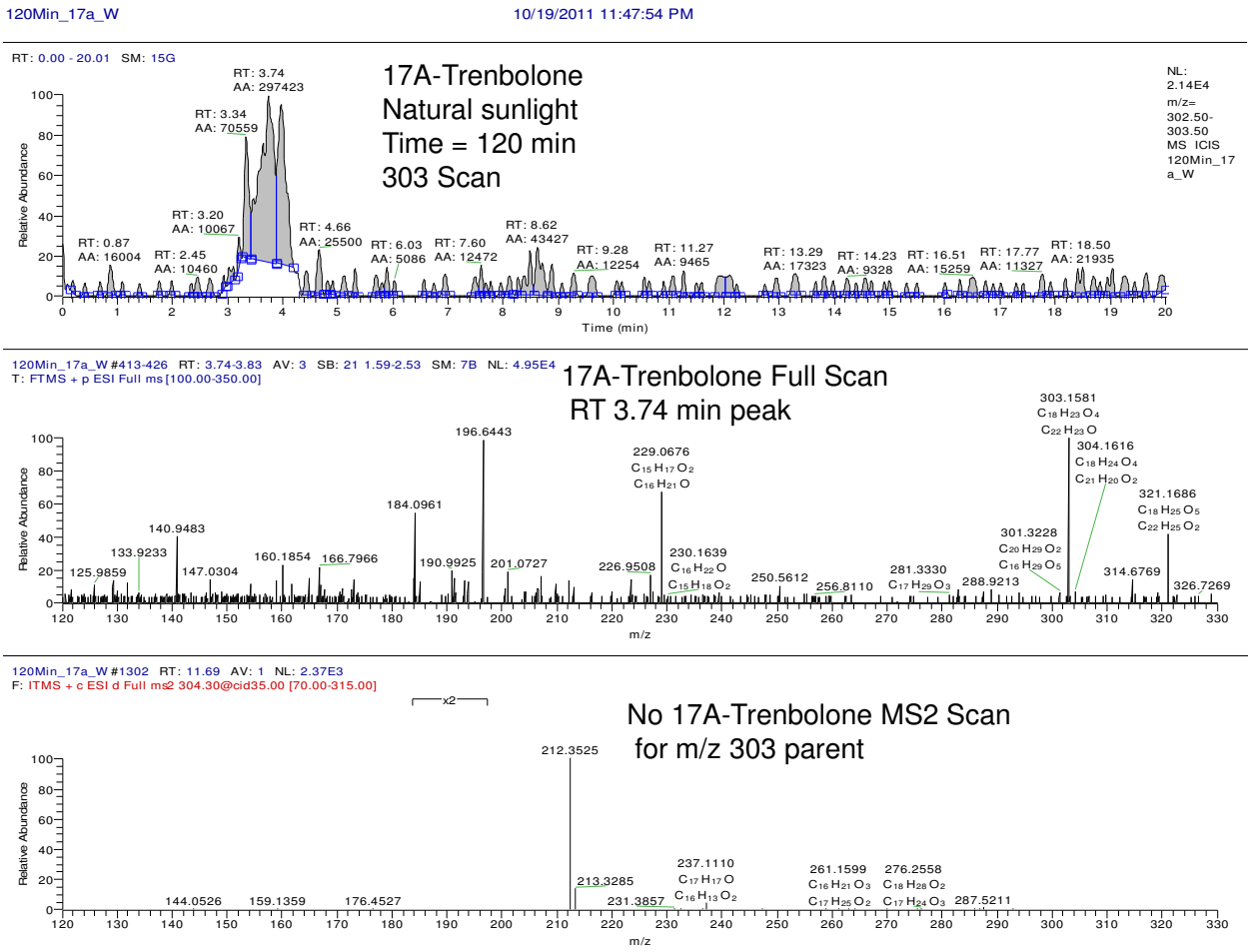

Figure S13: Observed 17α-TBOH product chromatogram and full scan spectra after 120 minutes of irradiation for the poorly resolved m/z 303 peaks observed at 3-4 minute retention times. As for 17β-TBOH, these peaks likely represent secondary and tertiary dialdehyde or dihydroxy products. No MS/MS spectra were collected for these particular products.

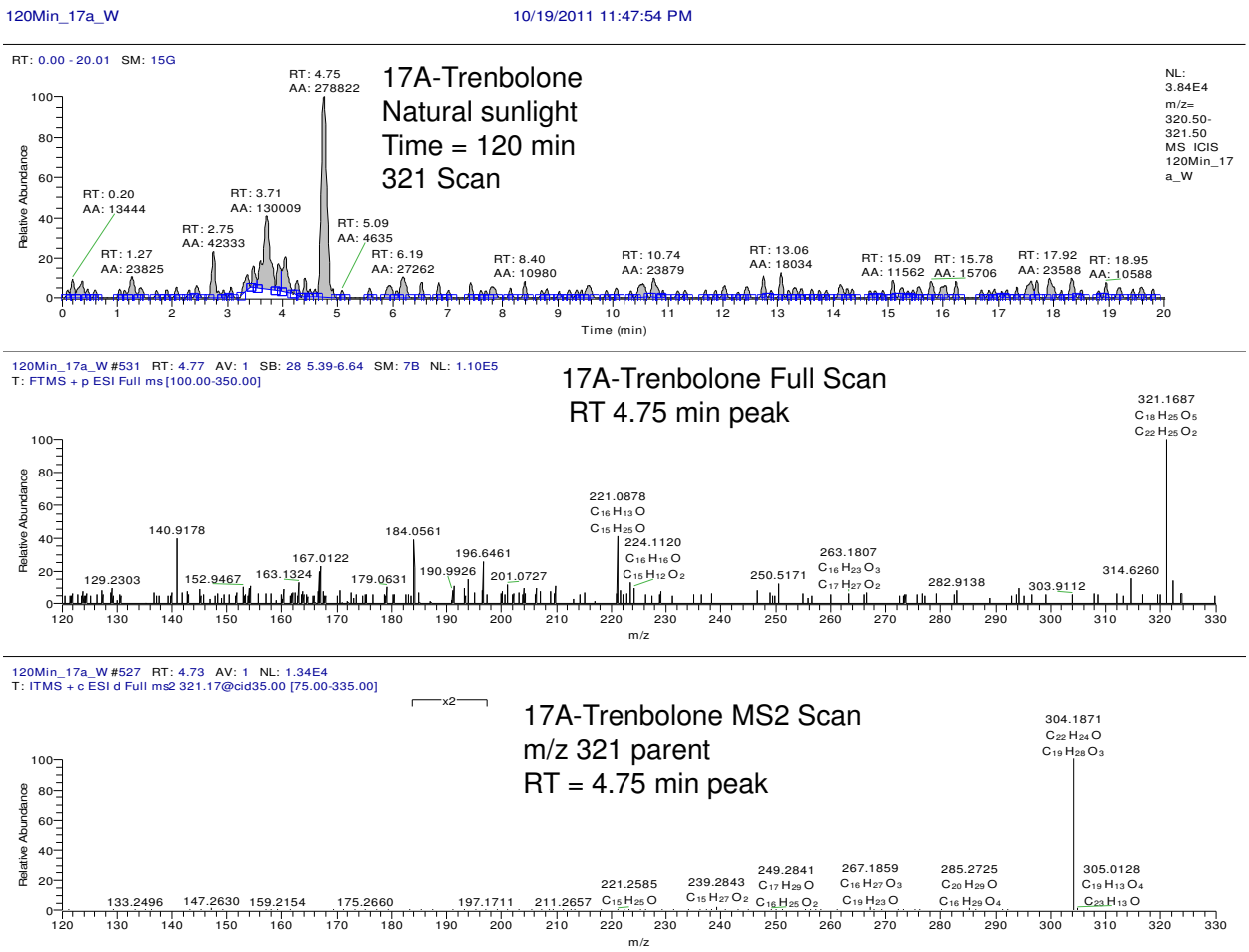

Figure S14: Observed 17α-TBOH product chromatogram, full scan spectra, and MS/MS spectra after 120 minutes of irradiation. The *m/z* 321 peaks at 3.71 and 4.75 minutes are presumably trihydroxy-trenbolone products.

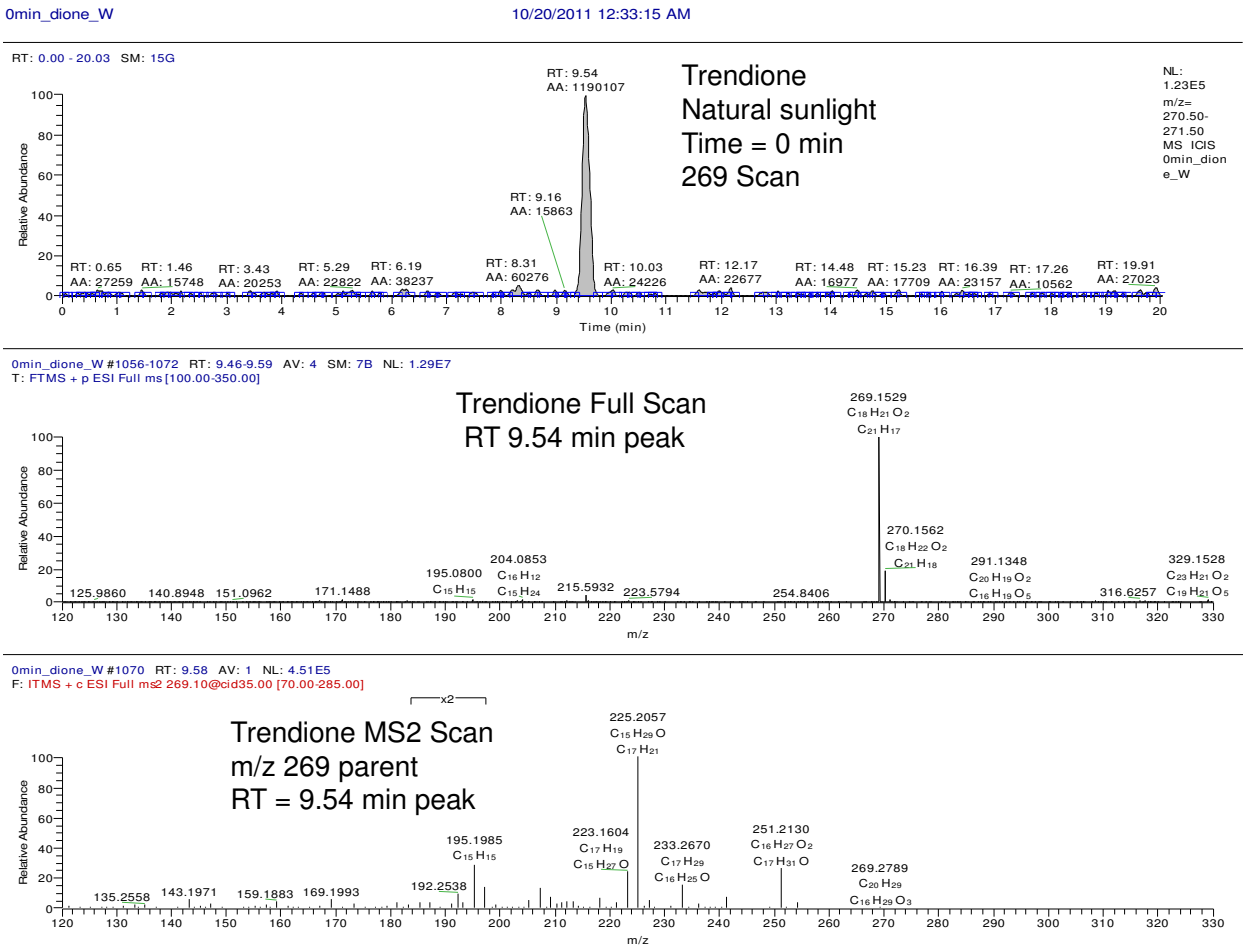

Figure S15: Initial TBO parent chromatogram, full scan spectra, and MS/MS spectra prior to initiating the photolysis experiment.

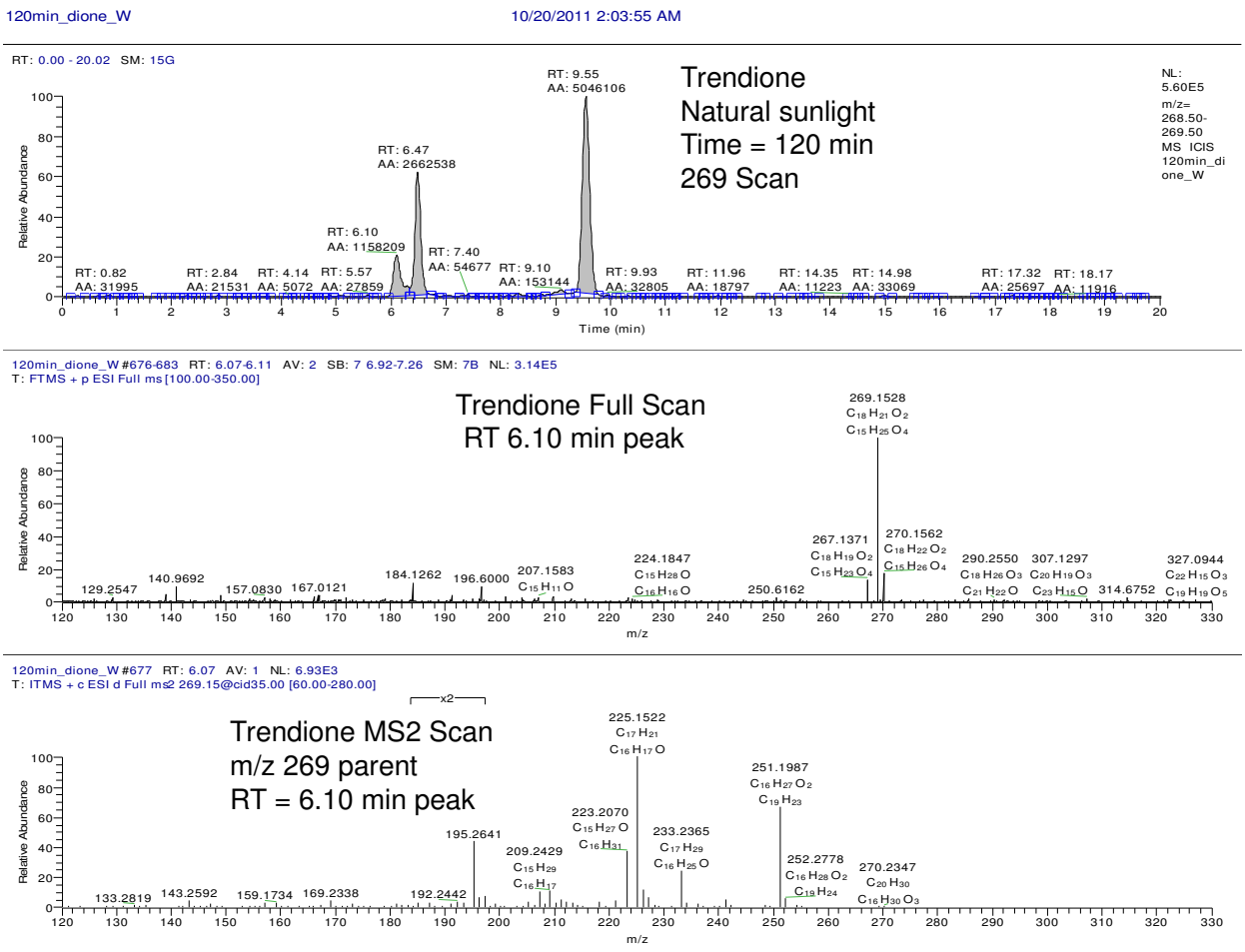

Figure S16: Observed TBO product chromatogram, full scan spectra, and MS/MS spectra after 120 minutes of irradiation for the *m/z* 269 peak at 6.10 minutes. Monohydroxy product peaks ($[M+H-H_2O]^+$ ions) are observed at 6.10 and 6.47 minutes. By analogy with 17β-TBOH products, we propose that the 6.47 minute peak is the dominant 12-hydroxy product for TBO, with the 10-hydroxy product at 6.10 minutes.

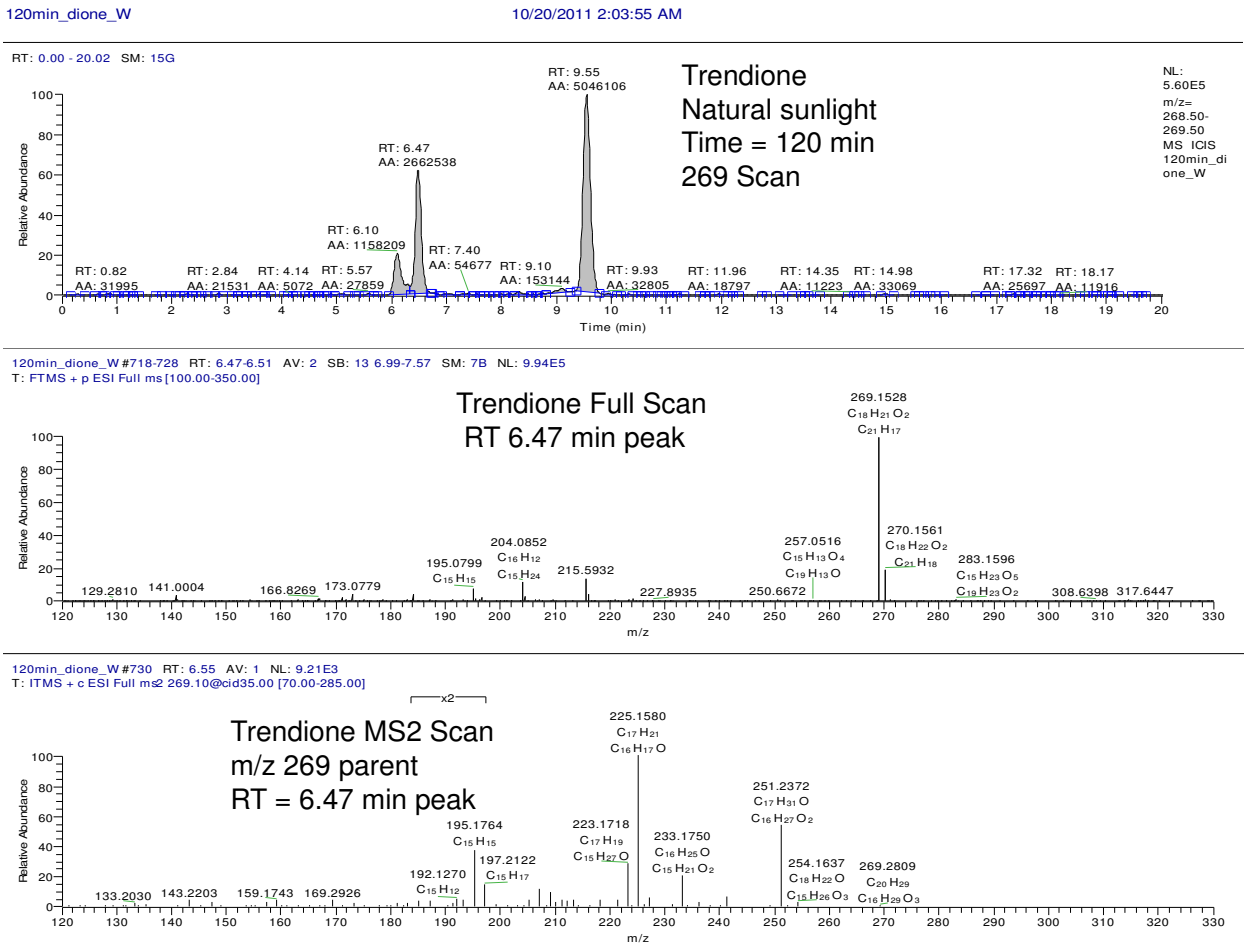

Figure S17: Observed TBO product chromatogram, full scan spectra, and MS/MS spectra after 120 minutes of irradiation for the dominant *m/z* 269 peak at 6.47 minutes. This is the dominant TBO photoproduct.

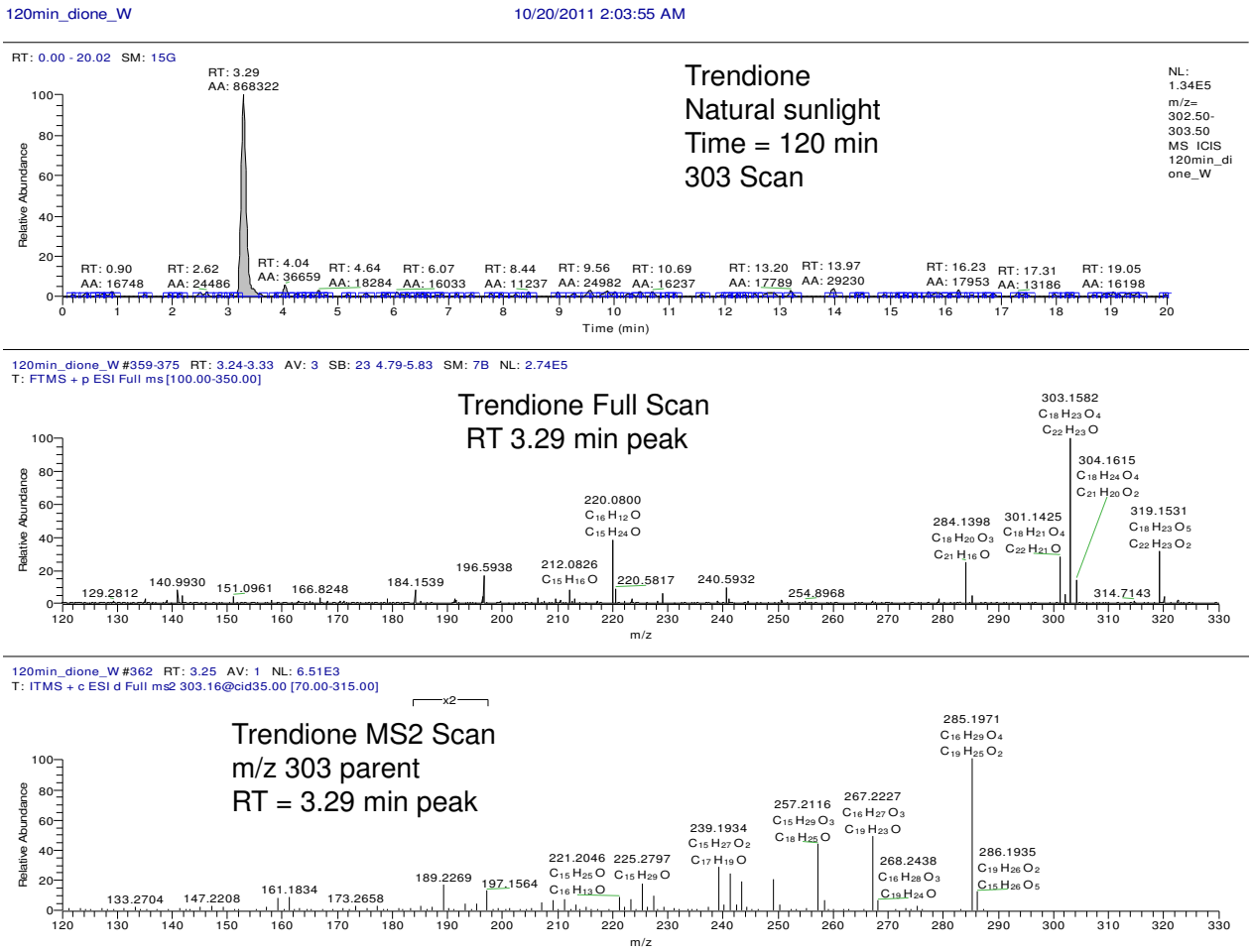

Figure S18: Observed TBO product chromatogram and full scan spectra after 120 minutes of irradiation for the *m/z* 303 peak observed at 3.29 minutes. As for 17β-TBOH and 17α-TBOH, this peak likely represents secondary or tertiary dialdehyde or dihydroxy products.

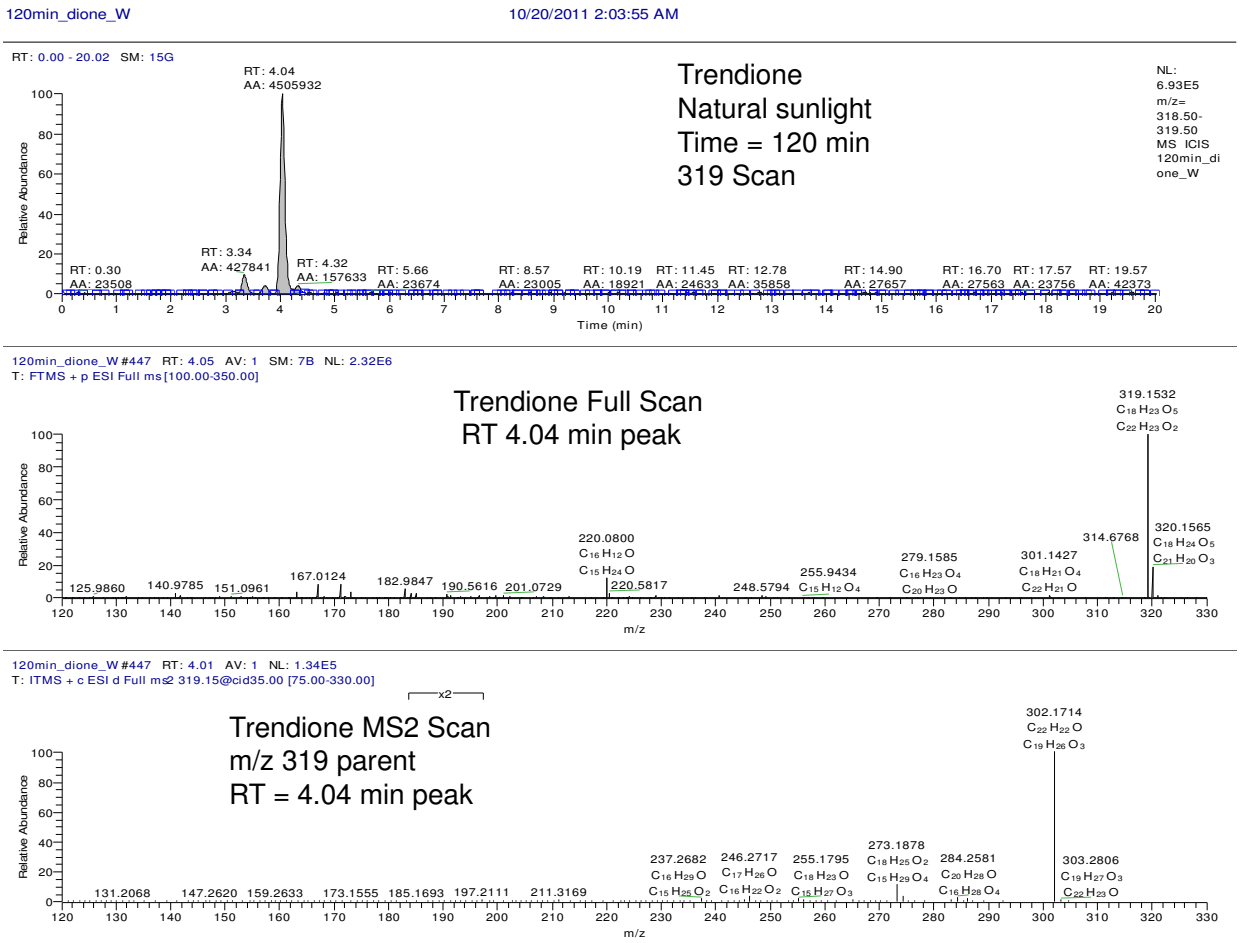

Figure S19: Observed TBO product chromatogram, full scan spectra, and MS/MS spectra after 120 minutes of irradiation. The *m/z* 319 peaks at 3.24 and 4.04 minutes are presumably trihydroxy-trendione products.

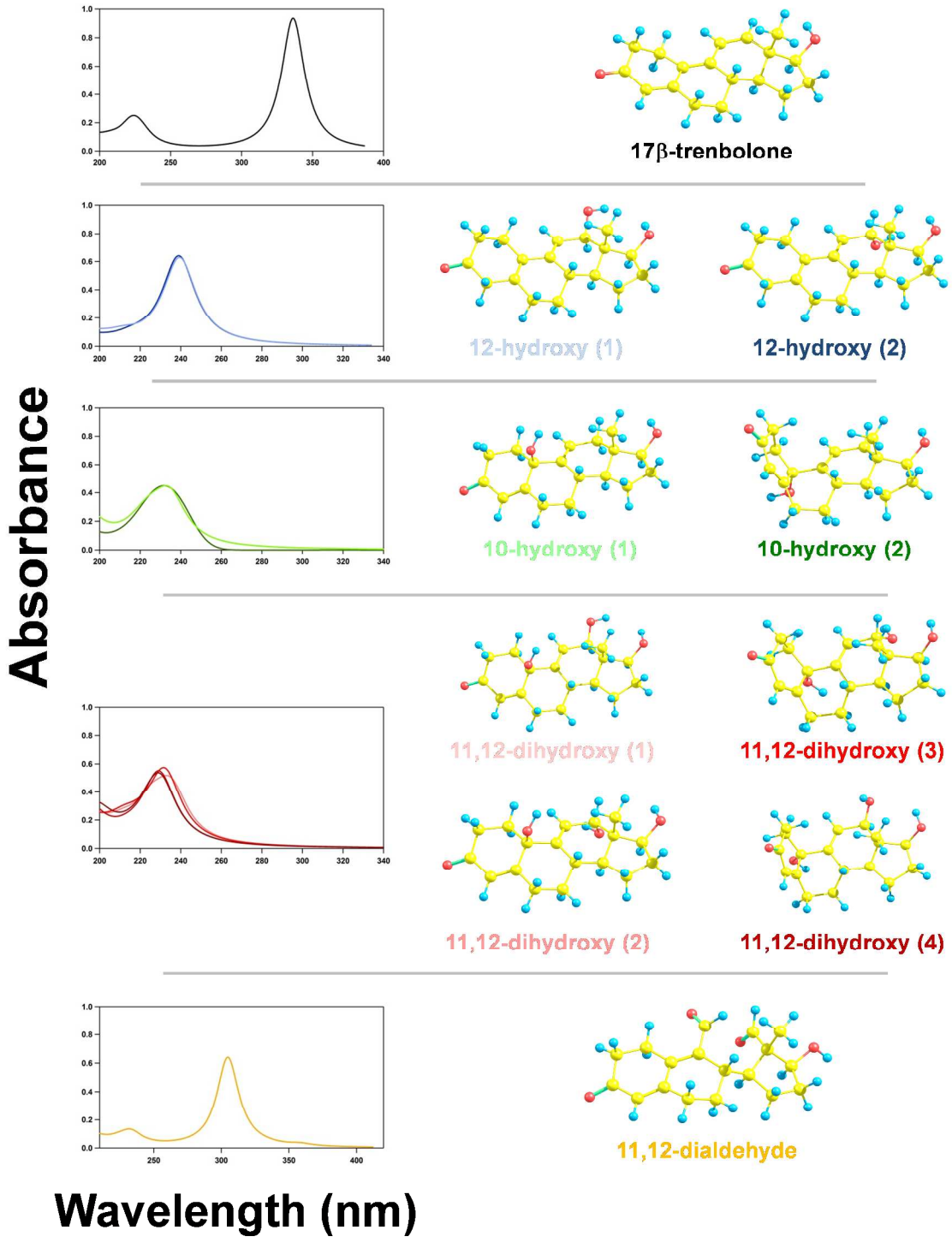

439

440 **Figure S20:** Calculated UV/vis absorbance scans for photoproducts of 17β-TBOH. Spectra are shown
441 for all possible stereoisomers, and the optimized structures from computational chemistry calculations are
442 provided. Aside from the 11,12-dialdehyde product, all photoproducts possessed similar absorbance
443 spectra. This prevented us from definitively distinguishing whether the two major products detected with
444 LC-DAD were diastereomers of 12-hydroxy or a mixture of 12- and 10-hydroxy species.

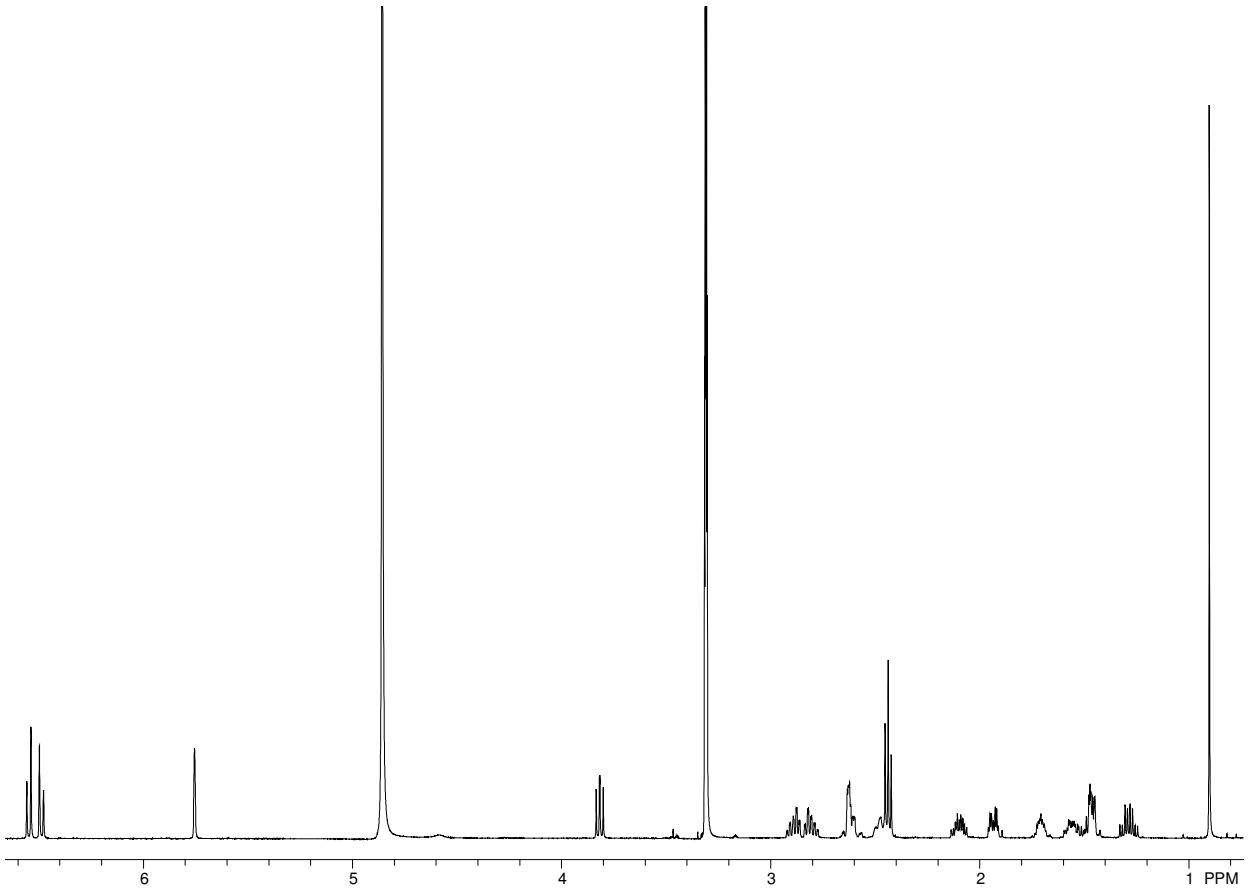

Figure S21: ^{1}H NMR Spectrum of 17β-TBOH in CD_3OD (500 MHz).

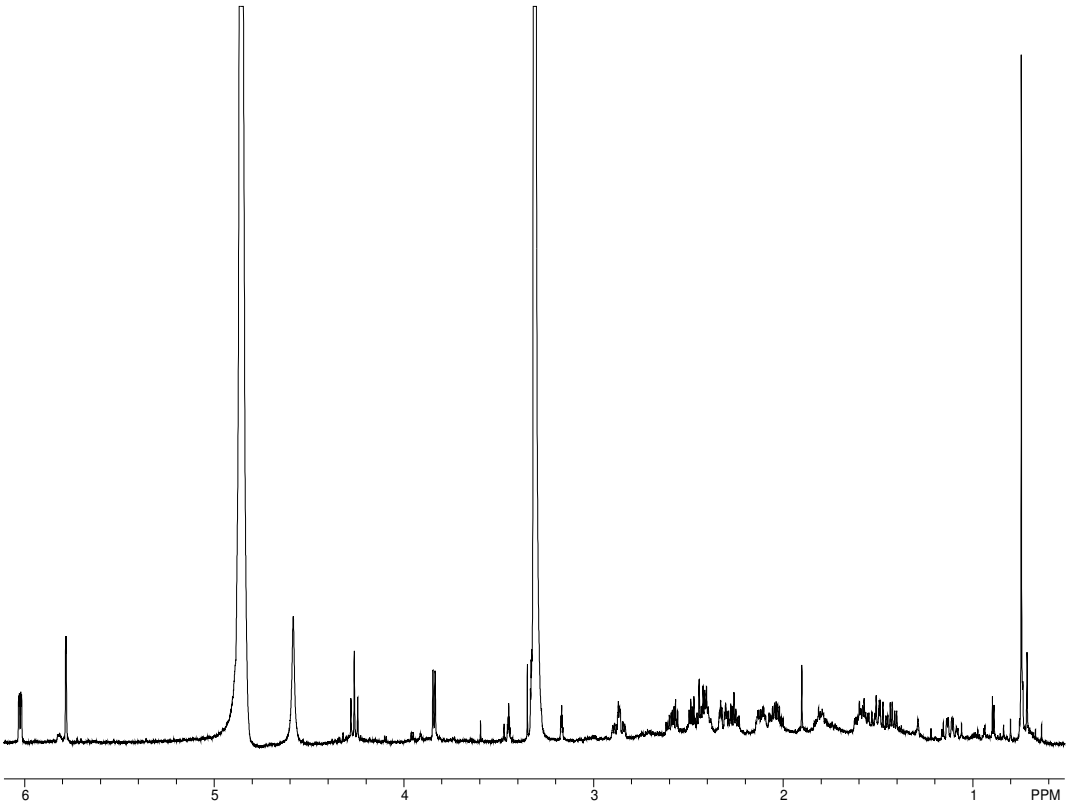

Figure S22: ^{1}H NMR Spectrum of 10,12-dihydroxy-trenbolone in CD_3OD (500 MHz).

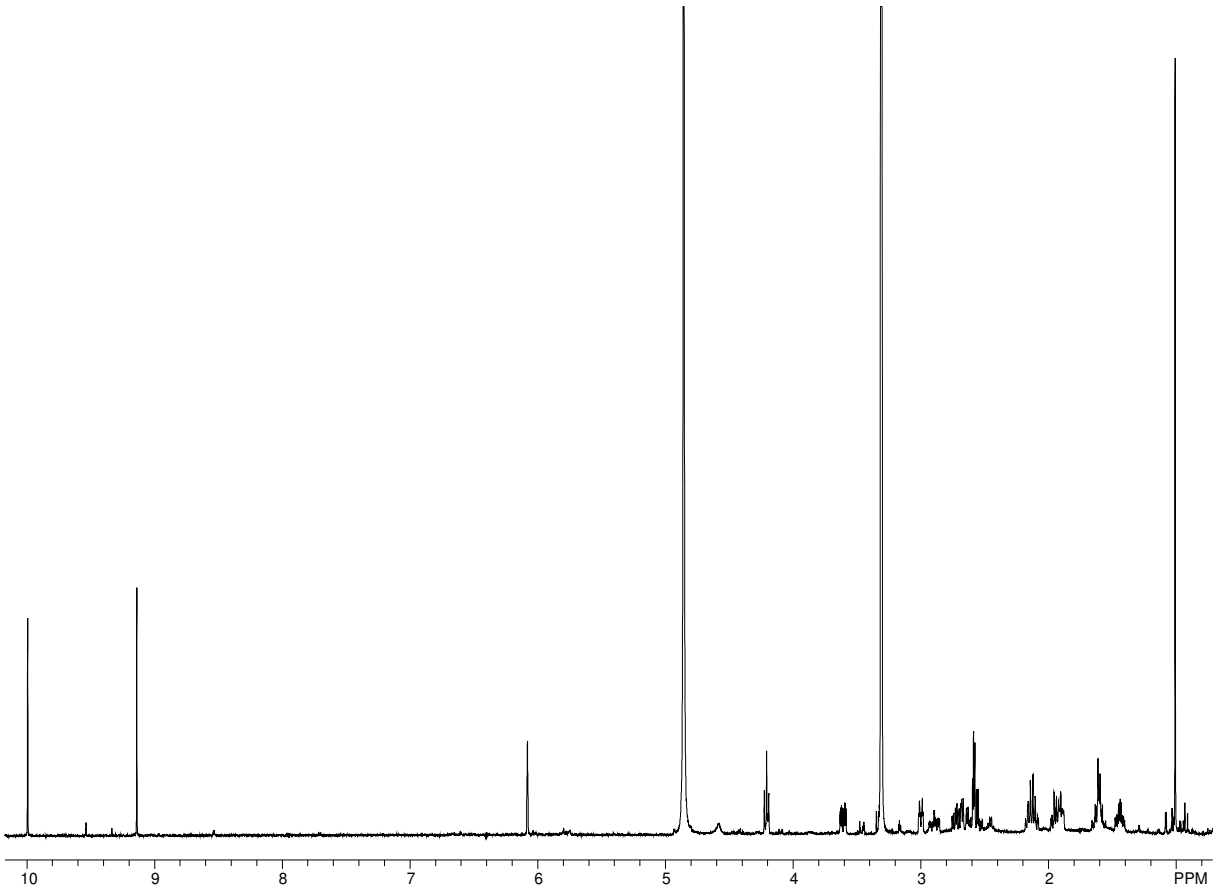

Figure S23: ^{1}H NMR Spectrum of 11,12-dialdehyde trenbolone product in CD_3OD (500 MHz).

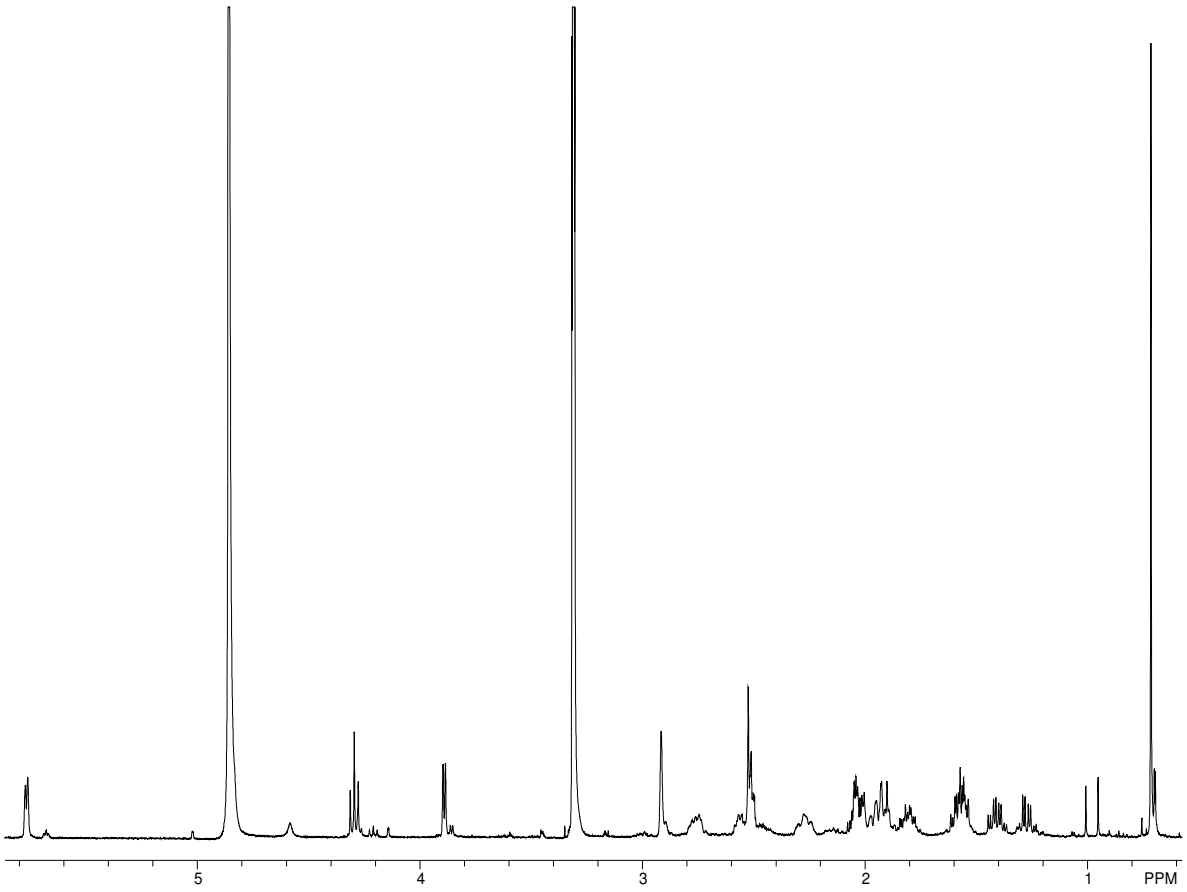

Figure S24: ^{1}H NMR Spectrum of 12-hydroxy-trenbolone in CD_3OD (500 MHz).

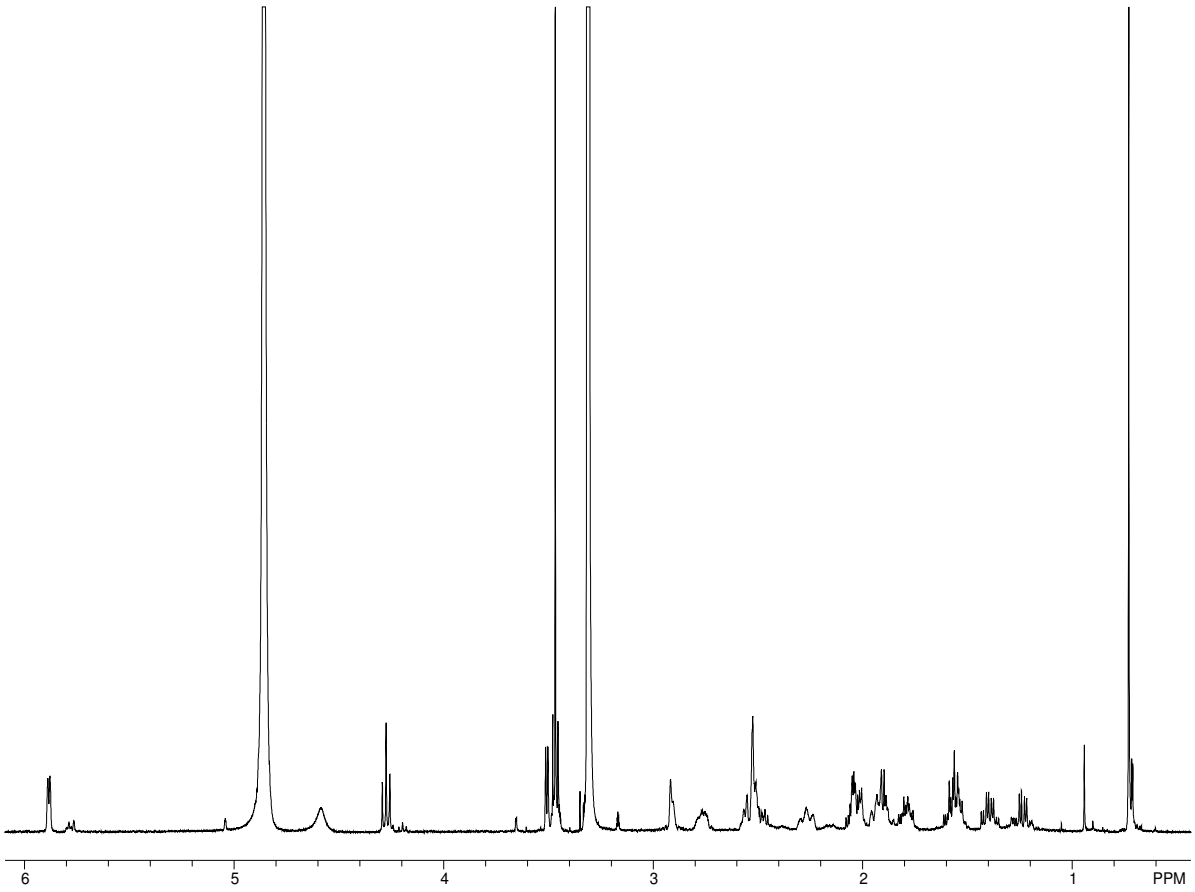

Figure S25: ^{1}H NMR Spectrum of 12-methoxy-trenbolone in CD_3OD (500 MHz).

Ecotoxicology Data

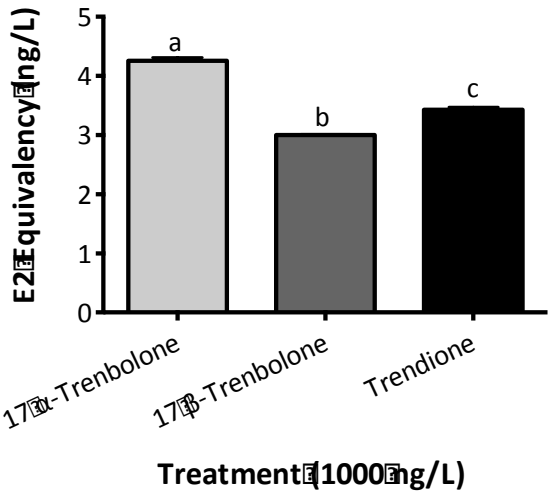

Figure S26: *In vitro* vitellogenin mRNA in rainbow trout hepatocytes after exposure to TBA metabolite photoproducts as a measure of mixture estrogenicity (ng/L; $p < 0.0001$). Data are shown as mean ± S.E.M.; different letters indicate significant differences. Also, the estrogenicity of 17α-TBOH and 17β-TBOH photoproduct mixtures were also significantly different from 17α-TBOH and 17β-TBOH parents.